European Journal of Taxonomy 861: 21–47
https://doi.org/10.5852/ejt.2023.861.2063
ISSN 2118-9773
www.europeanjournaloftaxonomy.eu
2023 · Véron B. *et al.*

Research article

New species of Pavlovophyceae (Haptophyta) and revision of the genera *Exanthemachrysis, Rebecca* and *Pavlova*

Benoît VÉRON [1,*], Etienne ROUGIER [2], Anthony TAYLOR [3] & Didier GOUX [4]

[1,2,3] Laboratoire de Biologie des Organismes et Écosystèmes Aquatiques (BOREA) Université de Caen-Normandie, MNHN, SU, UA, CNRS, IRD, 14000 Caen, France.
[1,2,3] Normandie Université, UNICAEN, UMR 8067 BOREA, MNHN, SU, CNRS, IRD-207, UA, 14000 Caen, France.
[3] Institute of Marine Sciences, University of Portsmouth, Portsmouth, Hampshire, UK.
[4] Normandie Université, UNICAEN, CMAbio3 (Centre de Microscopie Appliquée à la Biologie), SF EMerode, 14000 Caen, France.
[4] Normandie Université, ENSICAEN, UNICAEN, CNRS, UMR 6508 CRISMAT, 14000 Caen, France.

[*] Corresponding author: benoit.veron@unicaen.fr
[2] Email: etienne.rougier@gmail.com
[3] Email: anthony.taylor2590@gmail.com
[4] Email: didier.goux@unicaen.fr

Abstract. The justification of the 4 genera that currently compose the class Pavlovophyceae is based on a low number of species and a relative paucity of available, traceable and referenced cultures. Previous integrative phylogeny work revealed strains that can refine and strengthen our knowledge of the genera in the class. The application of multiple light and electron microscopy techniques allowed us to prioritize the cytomorphological characters (pyrenoid, thylakoid, stigma, knob-scales, life stage / life cycle) used for the taxonomy of these algae and to describe two new species: *Exanthemachrysis fresneliae* Véron sp. nov. and *Rebecca billardiae* Véron sp. nov. Consequently, revisions of the two genera *Exanthemachrysis* Lepailleur emend. Véron and *Rebecca* Green emend. Véron were made. In addition, the genus *Pavlova* Butcher emend Véron is revised in the light of these characters. Particular emphasis is placed on the life stages and habitat of the species.

Keywords. Haptophytes, phytoplankton, habitats, new species, pyrenoid.

Véron B., Rougier E., Taylor A. & Goux D. 2023. New species of Pavlovophyceae (Haptophyta) and revision of the genera *Exanthemachrysis*, *Rebecca* and *Pavlova*. *European Journal of Taxonomy* 861: 21–47.
https://doi.org/10.5852/ejt.2023.861.2063

Introduction

A need to explore the diversity of the Pavlovophyceae Green & Medlin came up after the last taxonomic review carried out by Bendif *et al.* (2011). This small class of phytoplankton is one of only three (i.e., Coccolithophyceae Rothmaler, Pavlovophyceae and Rappephyceae Kawachi, Kamikawa & Nakayama) currently recognized in the Haptophyta (Hibberd) Edvardsen & Eikrem which together represent unicellular

algae containing chlorophylls a + c and characterised by a filiform appendage called haptonema inserted between two unequal flagella (Parke *et al.* 1955). The recent revelation of a third class, the Rappephyceae within the phylum (Kawachi *et al.* 2021) shows that the biological diversity of the Haptophyta is still under-explored and thus under-estimated, only ca 330 described species are recorded in the modern ocean (Jordan *et al.* 2004; Eikrem *et al.* 2017) and as Edvardsen *et al.* (2000) concluded "there may be many novel as yet undescribed or unseen haptophyte taxa in the world's open ocean". Putative new lineages have been highlighted resembling those of the Pavlovophyceae (Simon *et al.* 2013; Egge *et al.* 2015).

The Haptophyta, as a major component of the pico- and nanoplankton, contains only few intensively studied species. No bloom of Pavlovophytes has ever been recorded and no toxic or even harmful episode has been registered. Members of the Pavlovophyceae are present in various habitats in nearshore environments, such as coastal and brackish waters, and also freshwater species or phylotypes have been identified or listed (Bendif *et al.* 2011; Shalchian-Tabrizi *et al.* 2011; Plancq *et al.* 2019). A seasonal preference for early spring and summer in the Skagerrak has been shown for some pavlovophytes (Egge *et al.* 2015). As pointed out by Not *et al.* (2012) the presence of Pavlovophyceae in open-ocean environments is uncertain and may be due to the difficulty in identifying them under light microscopes but in a later compilation of environmental sequencings (Edvardsen *et al.* 2016), it is clearly demonstrated that no operational taxonomic unit (OTU) corresponding to potential Pavlovophyceae comes from the ocean.

Despite being poorly explored, the Pavlovophyceae, mainly *Rebecca salina* (Carter) Green, *Pavlova pinguis* Green, *P. gyrans* (Butcher) Green & Manton and *Diacronema lutheri* (Droop) Bendif & Véron, are of major interest in supporting aquaculture production of bivalve larvae (Ponis *et al.* 2006) because of their high ingestibility and digestibility and the richness of their nutritional contribution in essential long chain polyunsaturated omega-3 fatty acids (docosahexanenoic – DHA and eicosapentaenoic – EPA).

In addition, the historicisation of fossil phenotypic traces and phylogenetic reconstructions tend to draw a tree of life in which the haptophytes occupy a singular place and where the Pavlovophyceae are close representatives of an ancestral haptophycean state after an evolutionary radiation which would have happened at the very early neoproterozoic (Strassert *et al.* 2021). It seems that they did not undergo significant effects during the K-Pg mass extinction, just like other soft-bodied haptophytes and this unlike the Coccolithales Schwarz (Eikrem *et al.* 2017). This difference in survival rate may be attributed to the mixotrophic capacity of some haptophyte lineages, which becomes a great advantage during the diminution in light intensity happening in the K-Pg mass extinction (Jones *et al.* 1994).

Bendif *et al.* (2011) carried out extensive integrative taxonomy of the Pavlovophyceae based on authentic type-strains (when still available in the collections, i.e., 10 out of 13) which increased the number of strains in culture within the Biological Resources Center of the Université de Caen Normandie, Algobank-Caen, reaching 29 in total (It should be noted that the term 'strain' is used here to refer to culture from single-cell isolate. The precision 'type-strain' therefore refers to the culture that was originally used to describe or emend a taxon). By combining molecular, pigmentary, morphological and ultrastructural characters, they confirmed the clear distinction between the four known genera corresponding to four clades, i.e., Clade 1 = *Exanthemachrysis* Lepailleur emend. Bendif & Véron, Clade 2 = *Rebecca* Green, Clade 3 = *Pavlova* Butcher emend. Bendif & Véron and Clade 4 = *Diacronema* Prauser emend. Bendif & Véron. They also highlighted many incertae sedis strains in the clades, some already appearing as new taxonomic entities to be studied.

In the genus *Exanthemachrysis*, after hesitation on its mono-specificity (Gayral & Fresnel 1979; Green 1980), it was confirmed that at present only *E. gayraliae* (Lepailleur) Bendif & Véron (culture AC15) is an authentic, traceable and studied strain (Lepailleur 1970). Other strains referenced and stored in the AC collection under codes AC35, AC37, AC245, AC246, AC249 and AC252 also belong to clade 1.

Within this monophyletic clade, a pigmentary complexity appears, since strains AC35, AC245, AC246 and AC249 have a type B profile (chlorophylls a, c1, c2, divinyl-chl-c, Mg-divinyl protochlorophyllide and with carotenoids ß-carotene, diadinoxanthin, diadinoxanthin-like, diatoxanthin, fucoxanthin), while strains AC15, AC37 and AC252 have type C profile (type B + monovinyl-chl-c). As suggested by Bendif *et al.* (2011) this difference in pigment composition corroborated by molecular phylogeny reveals at least two sub-clades, as long as type C profile is considered taxonomically reliable. In their phylogenetic tree, two unidentified morphologically similar strains (AC35 and AC245) appear genetically distinct from AC15, the type-strain of *E. gayraliae*. The strain AC35 is investigated here.

The genus *Rebecca* was separated from *Pavlova* (Edvardsen *et al.* 2000) and confirmed by Bendif *et al.* (2011) as a monophyletic clade. Although incompletely studied (van der Veer 1972) and the type-strain no longer existing in culture collections, Green transferred *P. helicata* van der Veer to this genus (Edvardsen *et al.* 2000). *Rebecca salina*, the only identified species, with a recorded and traceable type-strain (PLY465), was shown by Bendif *et al.* (2011) to individualise a sub-clade with another strain (PLY468), while a second sub-clade appeared in their tree with a single culture held in AC, strain AC537 that we therefore study here.

The historical genus *Pavlova* is currently reduced to three species i.e., *P. gyrans*, *P. pinguis* and *P. granifera* (Mack) Green by transfer of five species into the genus *Diacronema* with the work of Bendif *et al.* (2011). Their clade 3 is subdivided into two well separated sub-clades. It was shown that these sub-clades do not correspond to the three species studied from the authentic type-strains. In fact, the very homogeneous sub-clade 3.1 includes cultures referenced as type-strains *P. pinguis* (as CCAP940/2) and *P. gyrans* (as CCAP940/1b) showing same 18S rDNA and 28S rDNA sequences indicating a probable flasks mix-up. Recently Zhang *et al.* (2018) maintained the discrimination between the two species but the *P. gyrans* 18S rDNA sequences they reused came from strain CCAP940/1b (eq. to CCAP940/1B), from strain CCMP608 (referenced as a non-authentic type-strain) and from non-referenced *P. gyrans*, while none of the *P. pinguis* sequences they used correspond to authentic type-strains. We emphasise here the absolute necessity to use authentic type-strains, when available in culture collections, to ensure the robustness of phylogenetic studies. Although Zhang *et al.* (2018) clearly differentiate and confirm the two clades of *Pavlova*, their analyses do not invalidate the conclusions of Bendif *et al.* (2011) on the non-correspondence between the clades and these two species. It is noteworthy in Zhang *et al.* (2018) that both *Pavlova* sub-clades are not sister groups and the *P. pinguis*-like one is a sister group of the *Diacronema* clade. The question of the *P. gyrans* / *P. pinguis* complex therefore remains unresolved. On the other hand, the genetic distinction of the freshwater species *P. granifera* (strain PLY552) of clade 3.1 is indisputable as shown by Bendif *et al.* (2011), this species being the only authentic type-strain of sub-clade 3.2. The apparent genetic diversity of clade 3 suggests a cryptic diversity as emphasised by the authors, despite the absence of clear cytomorphological characteristics in the strains examined: AC19 was identified as *P. pinguis* by TEM (Billard C., pers. comm.) and AC33 is most likely a strain of *P. granifera* given TEM investigations (Billard C., unpubl. res.) and phylogenetic positioning close to strain PLY552. To further clarify the identity of the *Pavlova* sp. in sub-clade 3.2, we choose to examine the ultrastructure of strains AC248 and AC250 strains.

Diacronema is the richest genus in terms of species diversity. Clade 4 of Bendif *et al.* (2011) now gathers five well characterised species corresponding to traceable strains. Surprisingly, only few unidentified strains in collections supplement the five species, even though Egge *et al.* (2015) revealed four OTU's placed close by.

The use of several light and electron microscopy techniques allowed the strains to be compared with properly referenced species, leading to the description of two new species of the genera *Exanthemachrysis* and *Rebecca* and the subsequent revision of these two genera. The two other strains revealed a new strong cytomorphological character in the genus *Pavlova*, the ultrastructure of the pyrenoid which led to the revision of the genus.

Material and methods

Culturing method

Four marine strains *Exanthemachrysis* sp. AC35, *Rebecca* sp. AC537, *Pavlova* spp. AC248 and AC250 were isolated by J. Fresnel and obtained from AC (https://algobank.unicaen.fr) and grown in liquid medium in ES-Tris medium (Cosson 1987) and on 10% f/2 (Guillard & Ryther 1962) in agar on Petri dishes to stimulate the formation of benthic cells. The temperature was 20°C and illumination was provided by daylight fluorescent tubes at a photon flux of 30 µmol photons.m^{-2}.s^{-1} and a light/dark cycle of 12/12 h.

Light microscopy

In vivo light microscopy observations were performed with a Zeiss-AXIO Scope.A1 equipped with differential interference contrast (DIC) optics and photographed with an AxioCam MRc.

Transmission electron microscopy

Negative stain of whole-mounts

A droplet of the culture was put onto a glass slide and fixed by 1% osmium vapour for 5 minutes. Formvar coated grids were used to collect cells by sedimentation for 15 minutes. Excess culture medium was removed with filter paper. The grids were then negative stained with 1% uranyl acetate for 30 sec, dried and observed with a TEM JEOL JEM 1011 transmission electron microscope at CMABIO, Université de Caen Normandie, France.

Fixation methods

Cultures in liquid and on agar were prepared for thin section microscopy. Samples were fixed using two methods as described by Kawachi *et al.* (2021):

– Fixation method 1: one hour fixation with 2.5% glutaraldehyde in 0.1 M sodium cacodylate buffer (pH 7.2) containing 0.25 M sucrose at room temperature (20°C).

– Fixation method 2: five hours fixation with 0.1% osmium tetroxide and 2.5% glutaraldehyde fixation in 0.1 M sodium cacodylate buffer (pH 7.2) at 4°C.

The Fixation method 1 is recommended to observe preserved cells as it is considered to be a more conservative method with respect to osmolarity, whereas the second method (Fixation method 2) ensures the peeling of the plasmic membrane due to cells' osmotic reaction and allows observation of KS.

Thin sections

For the liquid culture, 5 ml of each strain were centrifuged 20 min at 400 rpm (eq. 20 G) using a Heraeus Biofuge. The supernatant was removed, then half the samples were fixed either by Fixation method 1 or 2. The colonies grown on agar were carefully picked-up together with a small part of their substrate, and then fixed using Fixation method 1. All samples were rinsed in sodium cacodylate buffer with 0.25 M sucrose added for samples that were fixed in Fixation method 1. Dehydration was performed in a graded alcohol series and ethanol was gradually exchanged for Epon resin (Emded 812 EMS). The pellets in resin were left overnight. The Epon resin was then exchanged again with fresh resin and left for 2 hours before the samples were placed into moulds and incubated at 60°C for 48 hours. Ultra-thin sections (80 nm) were made with a LEICA Ultracut R, placed on grids and double stained with 5% aqueous uranyl acetate and lead citrate before observation with the same TEM as the whole-mounts.

Scanning electron microscopy

7 ml of concentrated twice fixation solution (i.e., Glutaraldehyde 5% diluted in Sodium Cacodylate 0.2 M supplemented by 0.5 M of sucrose) were added to 7 ml of liquid culture in a 15 ml centrifuge tube. After one hour at room temperature, the tube was stored at 4°C for a week while cells sedimented

on Thermanox coverslips coated with L-polylysine. The sample was then dehydrated in a graded ethanol series and critical point dried (CPD 030 Leica).

Samples were then coated with platinum (JEOL JDC 1200) and observed with a ZEISS SUPRA 55 SEM at CRISMAT (Université de Caen Normandie, ENSICaen, CNRS).

Measurements

LM measurements were carried out with AxioVision software, while TEM and SEM pictures were analysed with ImageJ.

Type material deposition

The resin blocks used for this study were deposited in the CN herbarium under the codes specified in the holotype descriptions.

Abbreviations

AC = Algobank-Caen
AF = anterior flagellum
C = chloroplast
CCAP = Culture collection of algae & protozoa (Oban, UK)
CCMP = Culture Collection of Marine Phytoplankton (now National Center for Marine Algae and Microbiota, Bigelow, USA)
CN = Université de Caen Normandie Herbarium
E = eyespot (= stigma)
ER = endoplasmic reticulum
F = flagellum / flagella
Fix 1 = Fixation method 1
Fix 2 = Fixation method 2
G = Golgi apparatus
H = haptonema
KS = knob-scales
LM = light microscope
M = mucilage
N = nucleus
P = paramylon granule
PF = posterior flagellum
PLY = Culture collection of The Marine Biological Association (Plymouth, UK)
PY = pyrenoid
SEM = Scanning Electron Microscope
TEM = Transmission Electron Microscope
TH = thylakoid

Results

Strains AC35 and AC537 studied here, chosen according to their position on the phylogenetic tree of Bendif *et al.* (2011), turn out to be new species with specific cytomorphological characters. Their affiliation to genera is consistent in both cases but requires revision of both genera for precision and integration of the characters of these new species.

Taxonomic treatments

Phylum Haptophyta (Hibberd) ex Edvardsen & Eikrem
Class Pavlovophyceae Green & Medlin
Subclass Pavlovophycidae Cavalier-Smith
Order Pavlovales Green
Family Pavlovaceae Green
Genus *Exanthemachrysis* Lepailleur emend. Véron

Exanthemachrysis fresneliae Véron sp. nov.
PhycoBank: 103626
Figs 1–6

Diagnosis

The new species differs from the only species of the genus, i.e., *Exanthemachrysis gayraliae*, mainly by the presence of ovoid pedunculated knob-scales arranged helically on the AF but also by a slightly

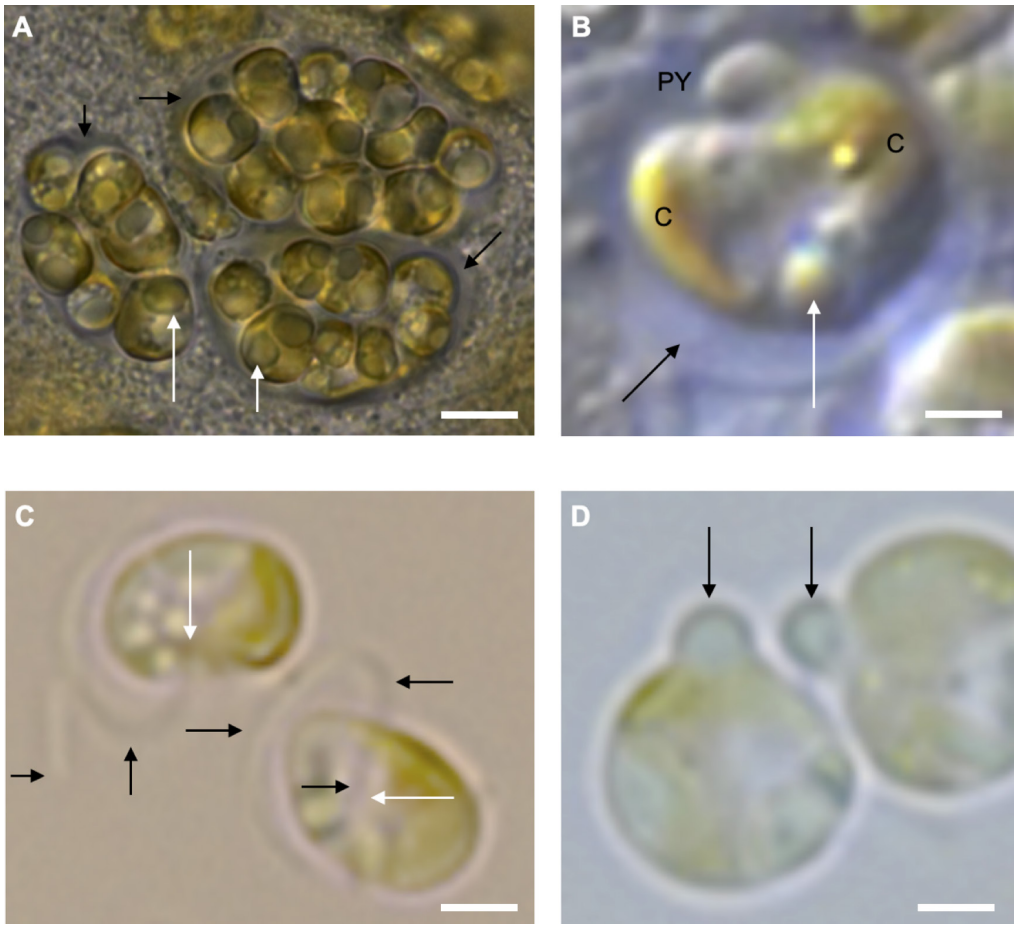

Fig. 1. *Exanthemachrysis fresneliae* Véron sp. nov. (AC35), palmelloid and swimming cells, LM images. **A**. Benthic colonies of non-motile sister cells embedded in non-stratified M (black arrows) with storage granules of P (white arrows). **B**. Benthic non-motile cell embedded in non-stratified M (black arrow) with storage granule of P (white arrow), bilobed C and anterior bulging PY. **C**. Apical view (bottom right) and side view (up left) of 2 swimming cells with conspicuous S-shaped AF (black arrows) emerging almost mid-ventrally from a pit (white arrows). **D**. Side view of motile cells with bulging PY (black arrows). Scale bars: A = 5 µm; B = 1 µm; C–D = 2 µm.

shorter AF. The benthic stage is pseudo-palmeloid. The pyrenoid is in *E. fresneliae* at the end of the C whereas it is in the centre of the C in *E. gayraliae*.

Etymology

The epithet given to the species is dedicated in honour of Dr Jacqueline Fresnel who worked at the Université de Caen Normandie, reinvestigated in details *E. gayraliae* and who described 22 taxa, mostly haptophytes.

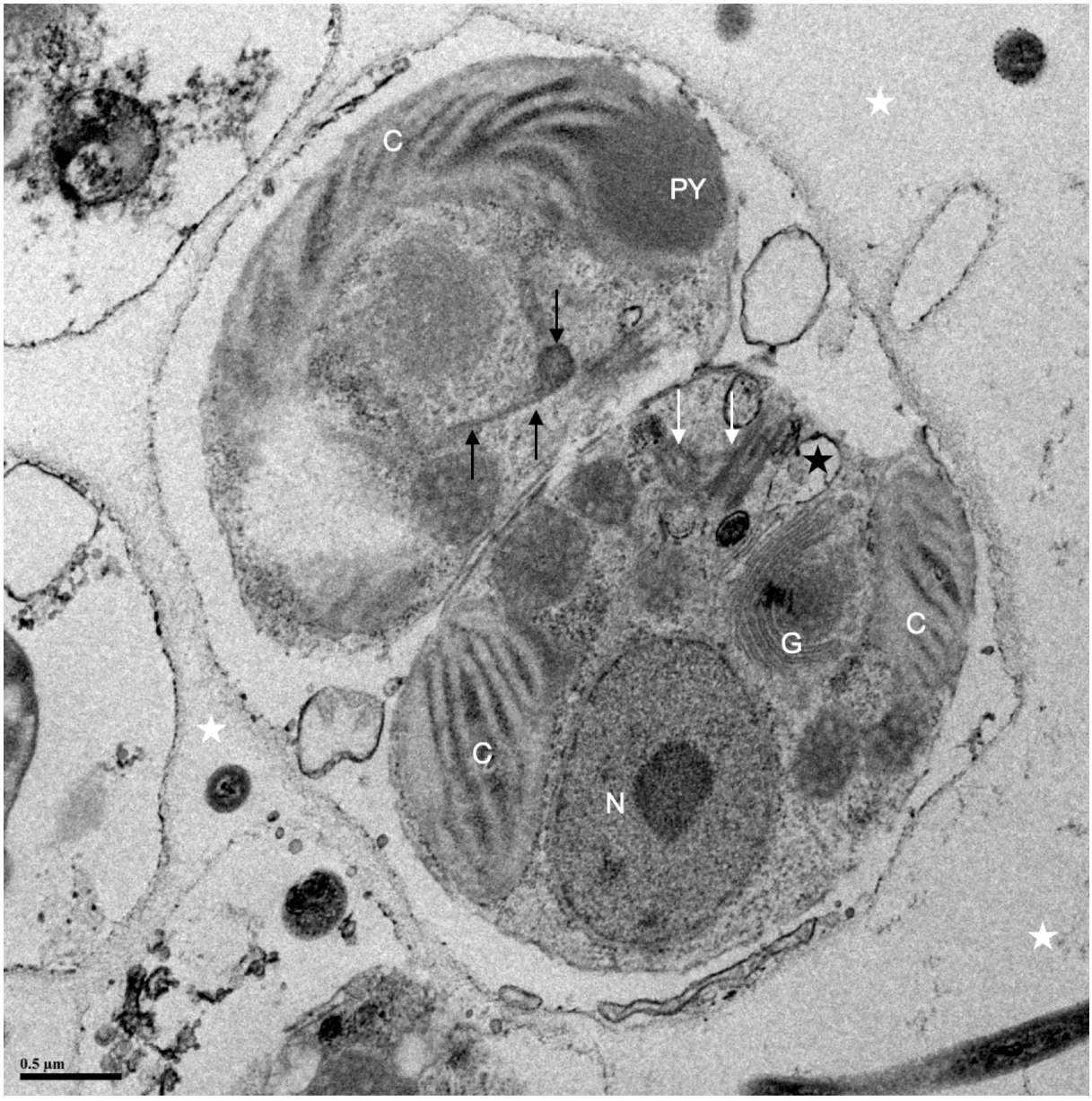

Fig. 2. *Exanthemachrysis fresneliae* Véron sp. nov. (AC35), palmelloid sister cells, TEM image (Fix 1). Benthic colony of non-motile sister cells embedded in a common non-stratified M envelope (white stars); parietal C with helicoidal arrangement of the TH lamellae and a bulging PY near the F bases perpendicular to each other (white arrows), with the basal bodies connecting to the microtubular root (black arrows) running to the central area of the cell. Secretory vesicles from G (black star) ready to discharge content near the pit where the F emerge. Scale bar: 0.5 µm.

Type material

Holotype

FRANCE • Normandy, Chausey Islands, Epi-silty; 48°52′ N, 1°49′ W; alt. 0 m; 1974; Jacqueline Fresnel leg.; Jacqueline Fresnel isol.; AC35; GenBank nos: JF714227, JF718767; CN[35NM1 – AC35-1M].

Description

Metabolic non-phototactic slightly bean-shaped motile cells. Single green-brownish chloroplast with a bulging PY, helicoidal and parallel thylakoids with an eyespot located at the thylakoids-pyrenoid interface. Sinusoidal anterior flagellum bears stalked knob-scales, rigid posterior flagellum with a long distal attenuation and a short haptonema. Cell membrane strewn with same shape and same size knob-scales.

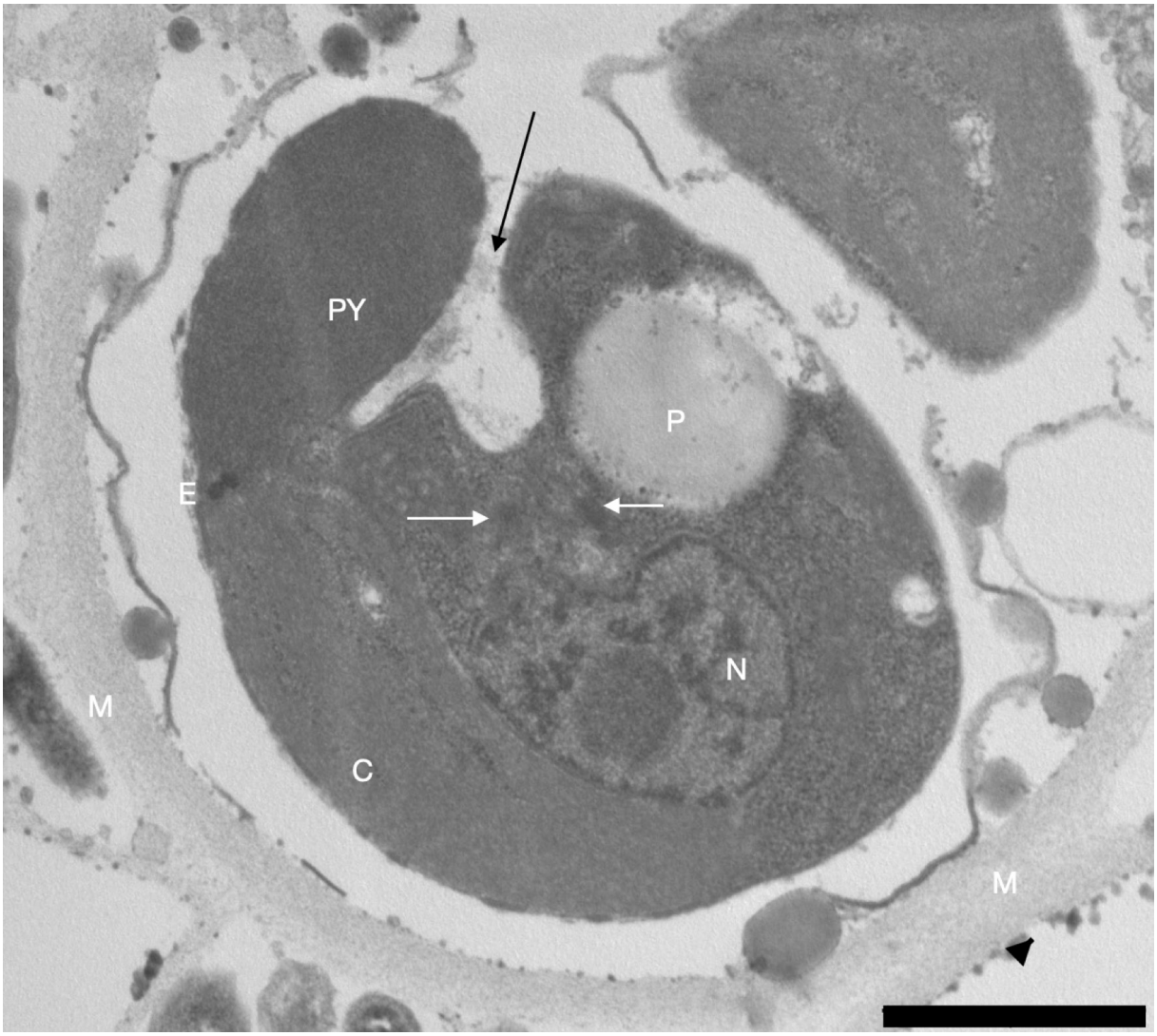

Fig. 3. *Exanthemachrysis fresneliae* Véron sp. nov. (AC35), palmelloid cell, TEM image (Fix 1). Non-motile benthic cell embedded in non-stratified M showing single parietal C with a bulging PY at its end. Row of few osmiophilic vesicles forming an E in C stroma located at the junction of TH and PY. Both F bases (white arrows) positioned in continuity with a notch in the nucleus facing the sub-ventral pit (black arrow). Scale bar:1 µm.

The non-motile palmelloid cells form colonies surrounded by non-stratified mucilage.

Microscopy and related analysis

The dominant stage is palmelloid with slightly ovoid cells (4.80 µm ± 0.57 × 4.21 µm ± 0.56, n = 51) forming colonies of sister cells remaining coated with a common non-stratified mucilage (Figs 1A–B, 2–3). Some cells can retain flagellar and haptonematal bases (Fig. 2).

Non-phototactic swimming cells have a marked flattened oval shape (4.69 µm ± 0.61 × 2.76 µm ± 0.35, n = 50) with an anterolateral pit giving a slight bean shape to the side-view (Fig. 1C). The parietal C is green-brownish (Fig. 1C) with helicoidal and parallel arrangement of TH (Fig. 2) and a bulging terminal PY (Figs 1–3) adjacent to a deep pit (Fig. 3). A discreet E is located on the outer periphery of the C between the chloroplast stroma and the PY (Fig. 3). The AF (approximately 8–9 µm) is covered by a layer of ovoid KS (42 nm × 37.5 nm) produced in the Golgi body (Fig. 5C) aligned in continuous helicoidal rows from the base (Fig. 4). The PF (about 5–6 µm) is composed of two parts of almost equal length. The proximal part, comparable in diameter to the AF, tapers into a thinner distal part and the H, regular in diameter, measures about 2–3 µm. All three appendages emerge at the surface of the cell from the pit (Fig. 5A–B). Both the PF and H, as well as the cell membrane, are sporadically covered with KS identical (Fig. 5C) to those present on the AF (Fig. 4A,C).

Taxonomic outcome: a revised description of the genus *Exanthemachrysis*

Due to the description of a second species in the genus *Exanthemachrysis*, a revision of the genus is necessary. The description based on *E. gayraliae* (Lepailleur) Bendif & Véron has become too general and can now be emended following the description of *E. fresneliae* sp. nov. and other Pavlovophyceae described since, providing information unknown in 1970.

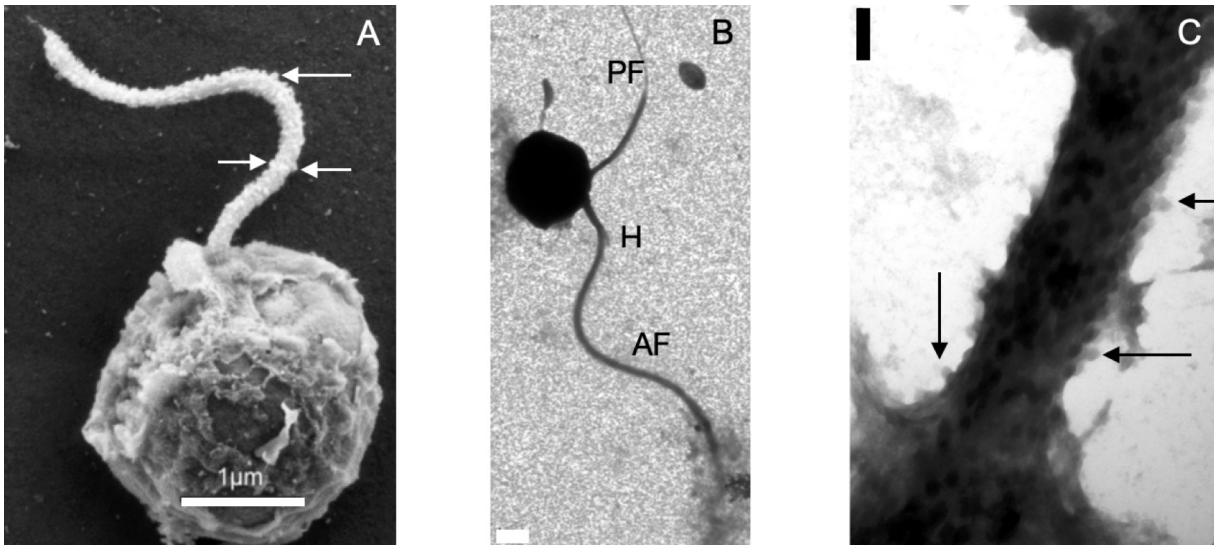

Fig. 4. *Exanthemachrysis fresneliae* Véron sp. nov. (AC35), flagellar apparatus of motile cells. **A**. SEM image of side view of swimming cell with a 3–4 µm long conspicuous sinusoidal S-shaped and slightly tapering AF emerging almost mid-ventrally and thickly covered by KS (white arrows). **B–C**. Negative staining image. **B**. Detail of the 3 appendices, the AF, the H and the PF composed of 2 parts of sub-equal lengths with a distal attenuation. **C**. Detail of the AF of a cell bearing ovoid KS (black arrows) down to the base, in regular helicoidal rows. Scale bars: A–B = 1 µm; C = 0.1 µm.

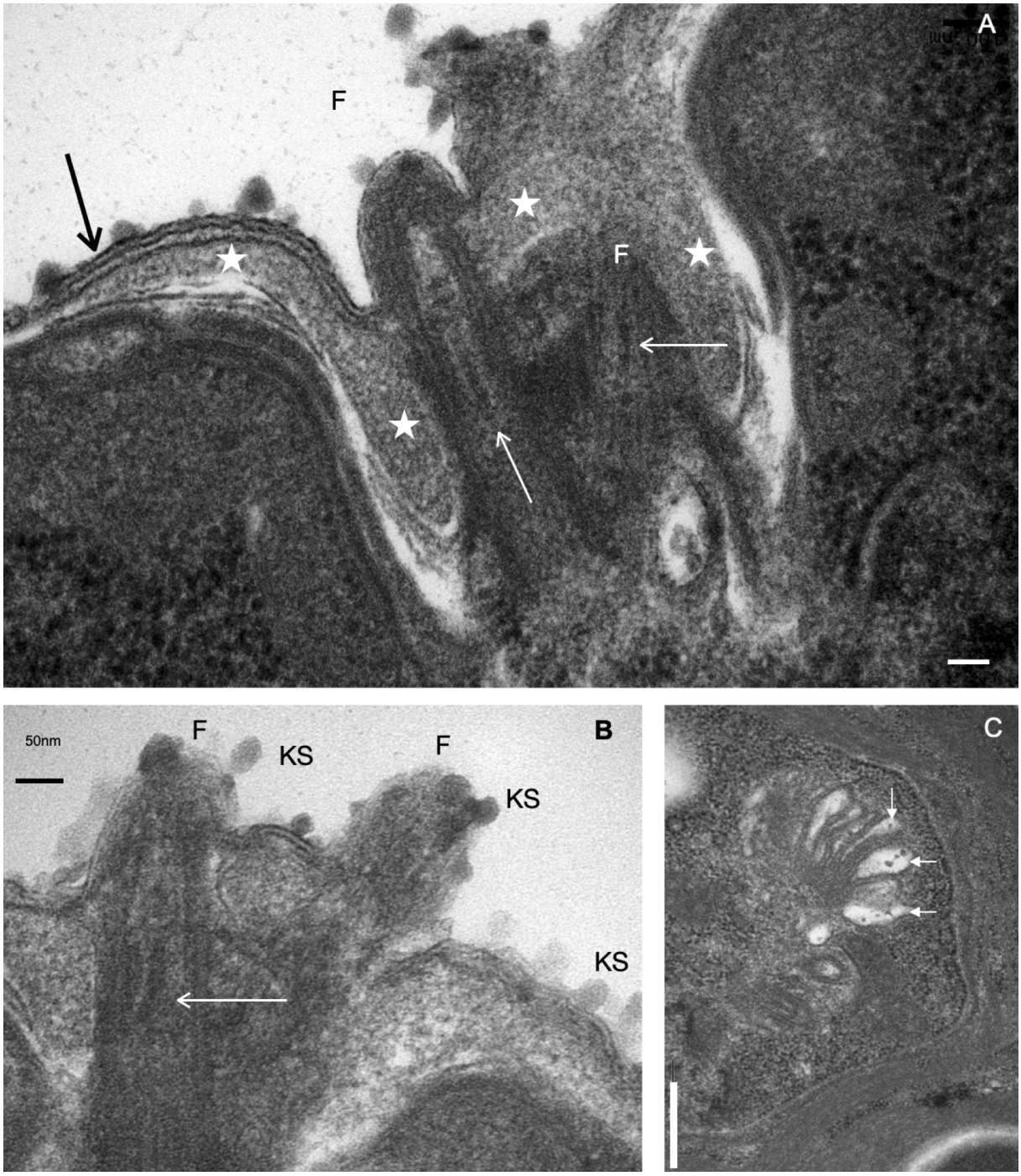

Fig. 5. *Exanthemachrysis fresneliae* Véron sp. nov. (AC35), flagella, plasma membrane and knob-scales, TEM images (Fix 1). **A**. Longitudinal section of the pit area with 2 emerging F (white arrows = central microtubules) surrounded by a sheath of reticulum enclosing their bases. Plasma membrane (black arrow), underlined with endoplasmic reticulum (white stars), covered with KS. **B**. Details of the cell surface in the region of F emergence. Oblique sections of F bases with central microtubules (white arrow). Stalked ovoid KS partially covering the F bases and the plasma membrane. **C**. G with cisternae and secretory vesicles containing KS (white arrows). Scale bars: A–B = 50 nm; C = 0.5 µm.

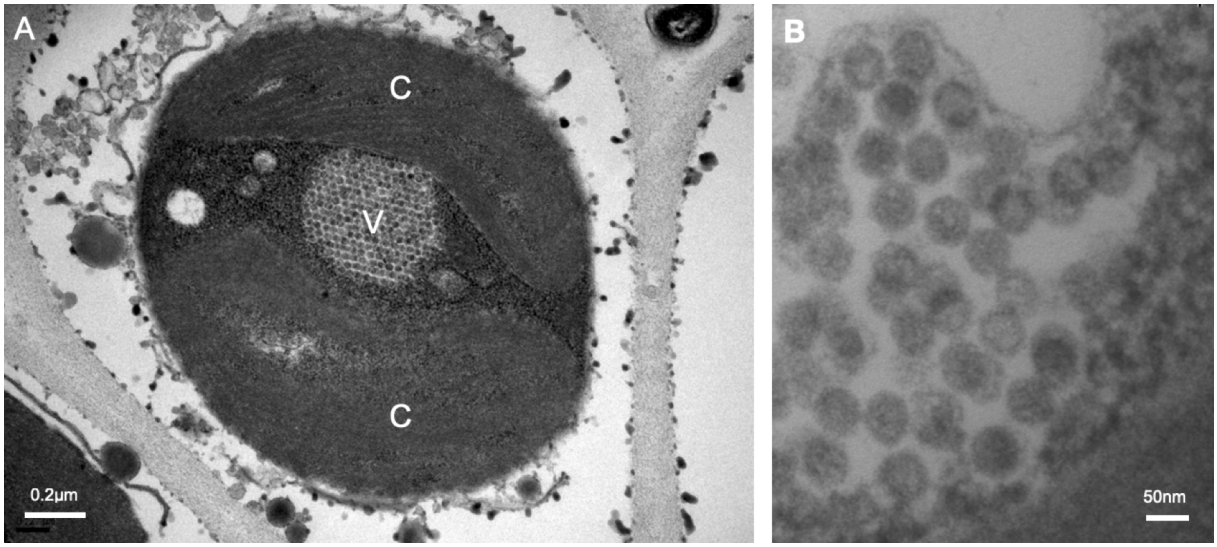

Fig. 6. *Exanthemachrysis fresneliae* Véron sp. nov. (AC35), viroplasm, TEM images (Fix 1). **A**. Benthic non-motile cell embedded in M; parietal C lobes with helicoidal arrangement of the TH lamellae. Cytoplasmic assembly of pentahedral virus (V). **B**. Viral particles scattered in the cytoplasm. Scale bars: A = 0.2 µm; B = 50 nm.

Exanthemachrysis Lepailleur emend. Véron
Figs 1–5

Included species

Exanthemachrysis gayraliae Lepailleur 1970: figs 1–4. – Bendif *et al.* 2011: fig. 4.

Exanthemachrysis fresneliae Véron sp. nov.

Emended description

Dominant stage of non-motile cells slightly ovate, embedded in mucilage. Brownish-green parietal chloroplast with a bulging pyrenoid forming an anterolateral protuberance on the cell body. Motile cells flattened oval, metabolic with three appendages. Distal attenuation of the bipartite posterior flagellum, haptonema short but not vestigial. Stalked ovoid knob-scales may be present. Anterolateral bulging pyrenoid, partially covering and bordering a pit where the flagella emerge, delimited from the chloroplast stroma by osmiophilic globules forming a stigma near the insertion of the appendages.

Genus ***Rebecca*** Green emend. Véron

Rebecca billardiae Véron sp. nov.
PhycoBank: 103627
Figs 7–9

Diagnosis

In addition to the very pronounced angular or even cubic and non-metabolic shape that the new species can take, *Rebecca billardiae* sp. nov. is also distinguished by knob-scales with only one constriction instead of two, and a slightly shorter AF.

Etymology

The epithet given to the species is dedicated in honour of Professor Chantal Billard who, from the 70s to the 2010s, worked at the Université de Caen Normandie. Chantal Billard described 29 taxa including many haptophytes and she notably described *D. virescens* (Billard) Bendif & Véron.

Type material

Holotype

FRANCE • Normandy, Baie des Veys, Canal de Carentan à la mer; 49°21′ N, 1°10′ W; alt. 0 m; 16 Feb. 2002; Fabien Jouenne leg.; Jacqueline Fresnel isol.; AC537; GenBank nos: JF714245, JF718773; CN[537-1NM].

Description

Motile cells not phototactic often ovate, some with strongly marked angular, even cubic forms. Less angular cells highly metabolic. Cell surface irregularly covered with stalked club-shaped knob-scales

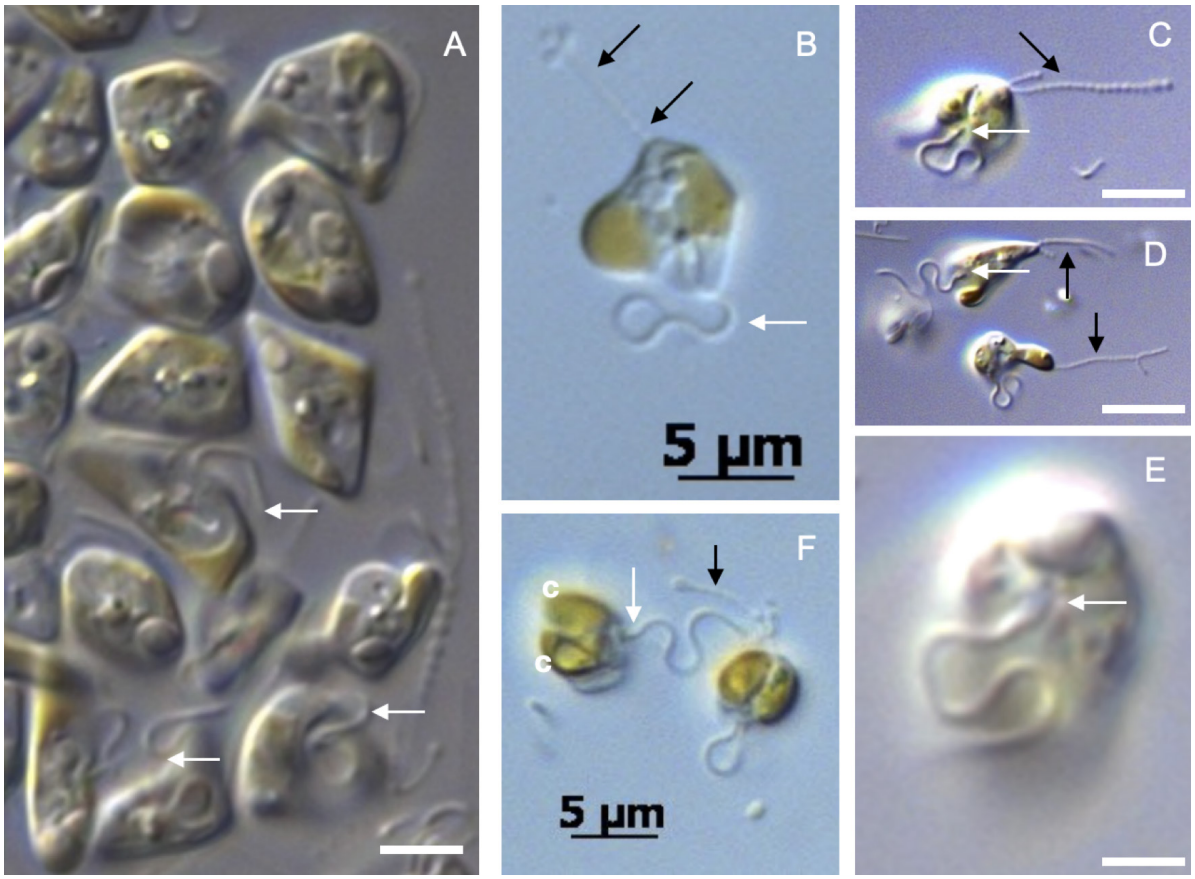

Fig. 7. *Rebecca billardiae* Véron sp. nov. (AC537), flagellate motile and non-motile cells, LM images. **A**. Gathering angular non-swimming flagellate cells with an S-shaped AF (white arrows). **B**. Polyhedral free-swimming cell with bilobed lateral golden-brown C, S-shaped AF (white arrow) and posterior beaded filipodium (black arrows). **C–D**. Cells of various shapes showing sub-apical insertion into a pit (white arrows) of the S-shaped AF. Posterior branched beaded filipodia present at the terminal part of the cell (black arrows). **E**. Ventral view of an angular free-swimming cell with sub-apical insertion of S-shaped AF into a pit (white arrow). **F**. Rounded cells with S-shaped sub-apically inserted AF (white arrow), posterior filipodium (black arrow) and bilobed golden-brown C. Scale bars: Scale bars: A = 4 µm; B–D, F = 5 µm; E = 1 µm.

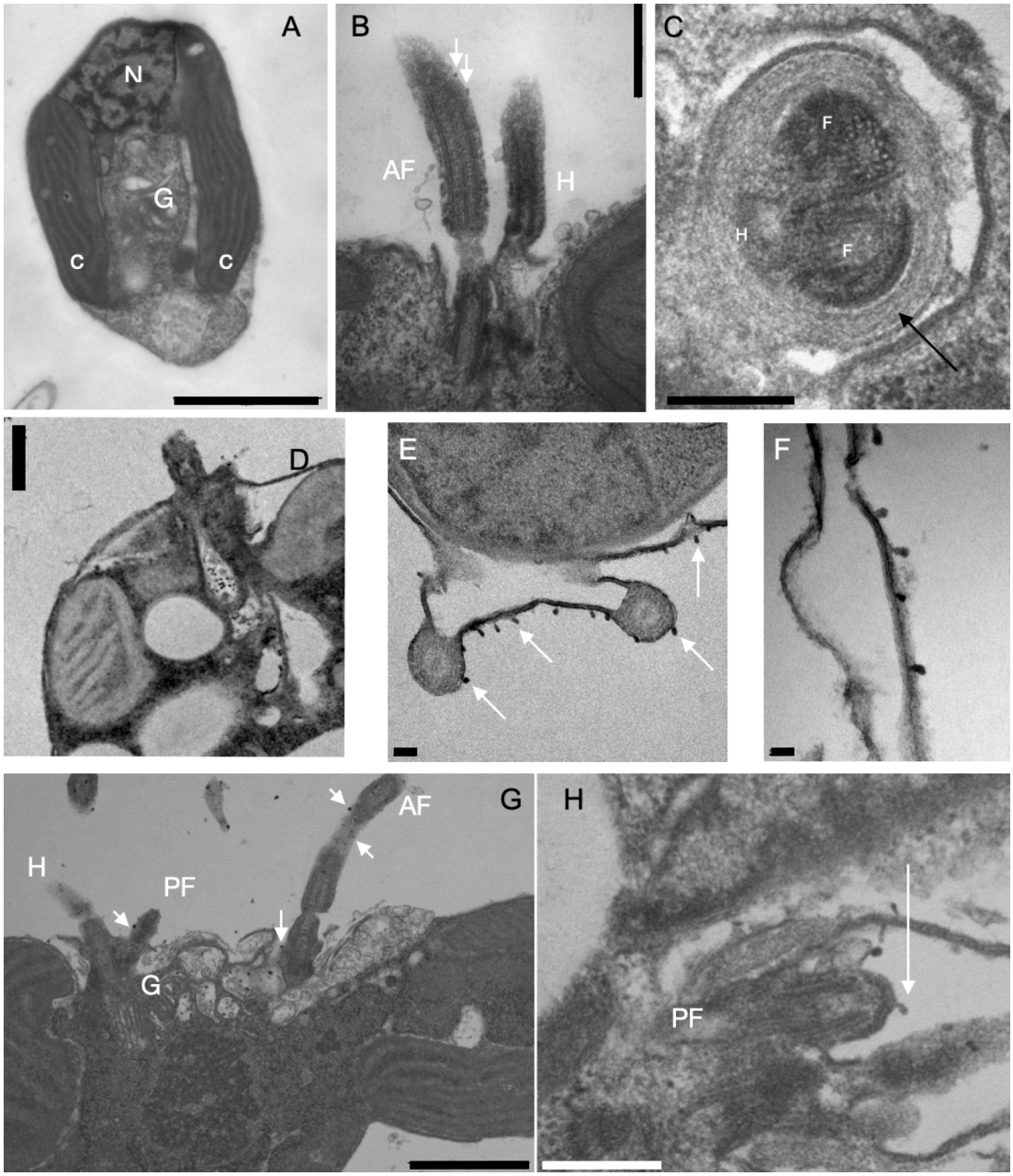

Fig. 8. *Rebecca billardiae* Véron sp. nov. (AC537), flagella, plasma membrane and knob-scales, TEM images (A–D, G–H = Fix 1; E–F = Fix 2). **A**. Angular cell with bilobed C and TH lamellae grouped by 3 sometimes twisted. **B**. Longitudinal section of a motile cell displaying the AF bearing few KS (white arrows) and the adjacent H. **C**. Cross-section of the sub-apical pit of a non-swimming cell containing the bases of H and F (transverse section – right, oblique section – left) sheathed by cytoplasm and surrounded by the plasma membrane (black arrow). **D**. Inflated G secretory vesicles unloading their materials including KS near the flagellar insertion zone. **E**. Periphery of a cell showing continuity of the plasma membrane along the curved AF, both covered with pedunculate KS (white arrows). **F**. Isolated plasma membrane retaining pedunculate mono-constricted club-shaped KS sporadically dispersed on its surface. **G**. Longitudinal section of a motile cell displaying the AF and PF both bearing few KS (white arrows) and the naked H. Note discharge of KS by G cisternae. **H**. Reduced PF cut in median longitudinal section showing microtubules and bearing a dense pedunculate club-shaped KS (white arrow). Central pair of microtubules is absent. Scale bars: A = 2 µm; B–D, H = 0.5 µm; E–F = 50 nm; G = 1 µm.

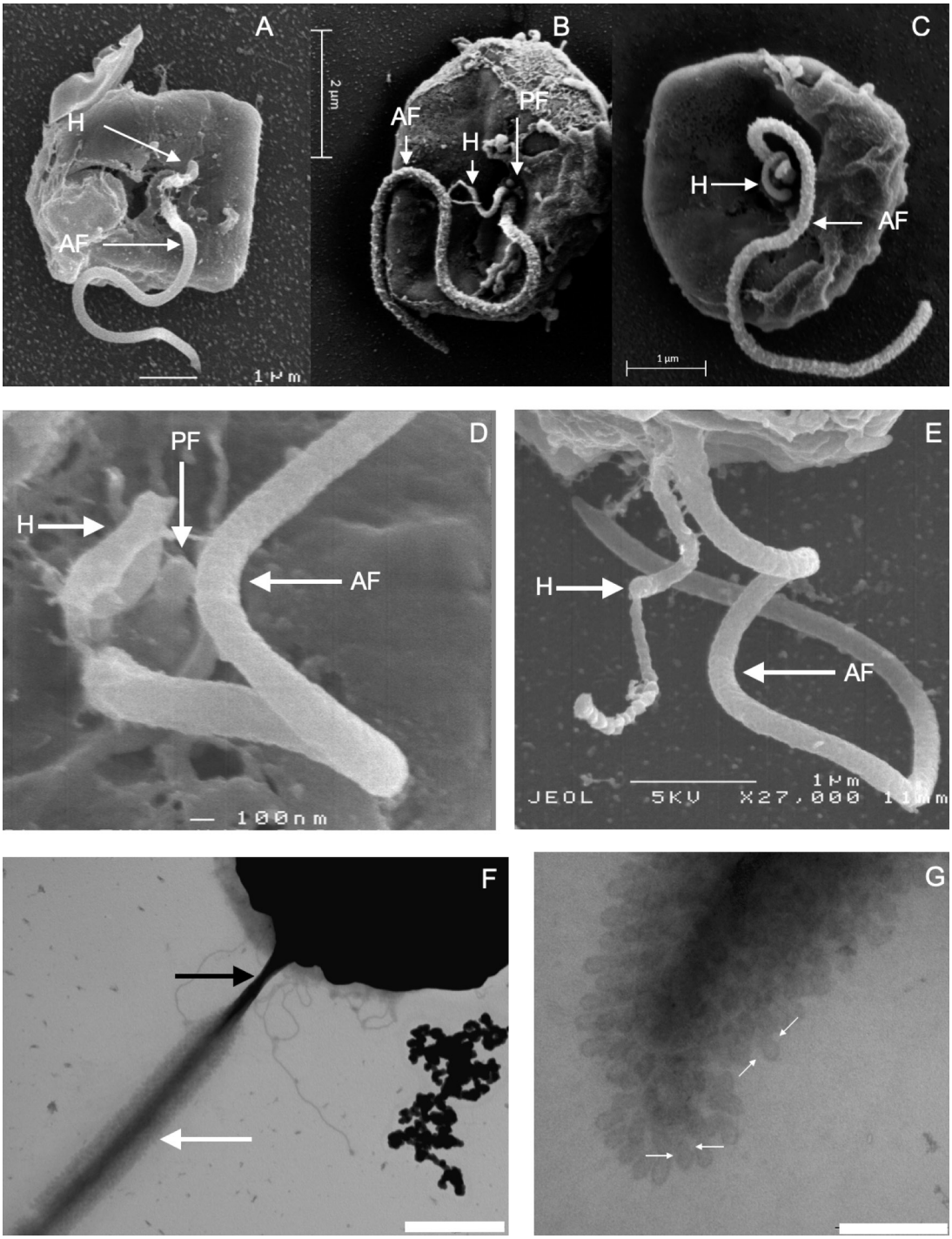

Fig. 9. *Rebecca billardiae* Véron sp. nov. (AC537), flagellar apparatus details of motile cells. **A–E**. SEM images. **A**. Ventral view of a cuboid cell with the S-shaped distally tapered AF and curved H. **B-C**. Ventral views of angular cells with the S-shaped AF covered with KS, the vestigial PF and the curved bipartite H between both F. **D-E**. Details of the insertion the 3 appendages. **D**. Vestigial PF. **E**. Bipartite H with the proximal hook-shaped half and the distal half forming a pearl string structure. Note distally tapered AF. **F–G**. Negative staining images. **F**. Proximal part of the tomentose AF with multilayered KS (white arrow), extending after a bare proximal zone (black arrow) in the immediate vicinity of the cell. **G**. Details of mono-constricted (white arrows) KS covering the distally attenuated AF. Scale bars: A, C, E–F = 1 µm; B = 2 µm; D = 100 nm; G = 200 nm.

with a single constriction. Single golden-brown bilobed chloroplast with parallel and helicoidal stacks of three thylakoids; pyrenoid and eyespot absent. Posterior filipodia branched and beaded. Sinusoidal anterior flagellum covered with a tomentum of knob-scales, proximal part remaining naked. Reduced posterior flagellum bearing few knob-scales. Naked bipartite haptonema with a proximal part of constant diameter and a string of pearl-like structures on distal part. Non-swimming cells gather with twisting anterior flagellum.

Microscopy and related analysis

After nearly two months of culture on agar plates, no colonies developed. Apparently only the flagellate stage exists in this species and consists of freely swimming cells. Often ovate (7.5 µm ± 0.6 × 6.1 µm ± 0.6, n = 50), cells can display very variable shapes, including cubic forms but mainly cells have flat unequal sides forming acute or obtuse angles at the circumference (Fig. 7A). When cells stop swimming, they gather, seeming to nestle together as closely as possible while keeping their long flagella beating (Fig. 7A). The appendages emerge from a sub-apical ventral pit (Figs 7E, 9A–E) surrounded at its base by a membrane sheath containing cytoplasm (Fig. 8C). There is a very clear difference between the three appendages present: the long wavy sinusoidal AF measures between 9 and 17 µm (13.6 µm ± 3.7, n = 17) and is covered, except at its base, by a thick fluff of mono-constricted KS (45 nm × 22 nm, n = 2) (Fig. 9F–G), at the tip it is tapered. The PF is atrophied forming a ≈200 nm high hump (Figs 8H, 9B, D). The H is well developed (3.0 µm ± 0.6, n = 8) and consists of two sections of almost equal length, the proximal part being of constant diameter, in the shape of a twisted hook (Fig. 9A–E), while the distal part, smaller in diameter, presents regular constrictions with the appearance of a pearl necklace (Fig. 9B, E). The two flagella as well as the cell body (Fig. 9C, E–G), but unlike the H, are covered with knob-scales in the form of pedunculated and clavate structure with a single median constriction (Figs 8E–F, 9G). The scales are sporadically distributed on the plasmic membrane and on the diminutive PF while on the long AF they may form a thick tomentum of several layers of lines oriented perpendicular to the flagellum axis and forming regular rows (Fig. 9F–G). On their posterior end, the cells develop beaded and branched filipodia often of great length, as long as the cells or the AF, and appearing to trail behind the cells (Fig. 7B–D, F).

Taxonomic outcome: a revised description of the genus *Rebecca*

Although retaining the basic characters of the genus *Rebecca*, the species described here, *Rebecca billardiae* Véron sp. nov., requires emendation of the description given by J.C. Green in Edvardsen *et al.* (2000).

Rebecca Green emend. Véron
Figs 7–9

Included species

Rebecca salina (Carter) Green 2000. – *Nephrochloris salina* Carter 1937: pl. 2, figs 10–22. – *Pavlova mesolychnon* van der Veer 1969: figs 1–21. – *Pavlova salina* (Carter) Green 1976: pls. 1–2.

Rebecca helicata (van der Veer) Green 2000. – *Pavlova helicata* van der Veer 1972: figs 1–8.

Rebecca billardiae sp. nov.

Emended description

Cells solitary, free-swimming, sometimes immobile, elongated and slightly compressed or angular to almost cubic, with two unequal flagella and short haptonema. Longer anterior flagellum with fine non-tubular hairs, posterior flagellum vestigial. A pit or canal penetrating the cell near the long anterior

flagellum. Clavate or mono-constricted scales on the cell body and rows of di- or trimeric scales on the anterior flagellum. Pale yellow-green to golden-brown bilobed single chloroplast with parallel and helicoidal thylakoid arrangement, stigma and pyrenoid absent.

Genus ***Pavlova*** Butcher emend. Véron
Figs 10–13

The unidentified strains of *Pavlova* (AC248 and AC250) were chosen for study because none had ever been examined within the sub-clade 3.2 (Bendif *et al.* 2011); both strains were found to have the same cytomorphological characteristics as the genus *Pavlova*.

Description of strains AC248 and AC250

Non-motile cells are occasionally present in cultures, clustered to a few in a loose mucilage (Fig. 11A) and showing a reduced flagellar appendage. Motile cells are slightly ovoid (5.9 µm ± 0.5 × 5.2 µm ± 0.4, n = 49), free swimming and highly metabolic (Fig. 10). Emergence of the appendages is from a narrow, shallow sub-apical pit (Fig. 12A). Except at its base (Fig. 12E), the AF (9.5 µm ± 3.8, n = 12) is coated with several layers of regularly spaced (Fig. 12D) flat and ovoid KS (≈47 × 34 nm, n = 4) with a slight median constriction and with fine non-tubular hairs (Fig. 12C). The smooth and short PF (1.9 µm ± 0.5, n = 6) is tapered distally (Fig. 12B). The bipartite H (1.1 µm ± 0.2, n = 7) consists of a proximal part of constant diameter and a distal part of equal length and smaller diameter. The single cup-shaped parietal C (Fig. 11B) contains bundles of thylakoids grouped in stacks three to five (Fig. 11C). One end of the C, near the pit and F bases, contains a conspicuous orange E (Fig. 10A–B) consisting of a cluster of osmiophilic globules located along its inner surface (Fig. 11B, D). In the centre of the C, opposite the F base, is a PY forming an ovoid bulge at the cell surface (Figs 10C, 11B, 12A). In transverse section, this protruding PY has the unusual aspect of a thick, wide utricle (Fig. 13A–B, D) curving in on itself (Fig. 13B–C) and entirely surrounded by the C-membrane bordered by the periplastic ER.

Details of the pyrenoid of *Pavlova* spp.

This particular form of PY, present in strains AC248, AC250 and also AC33 (Fig. 13D), had previously been observed in various species of *Pavlova* (i.e., *P. pinguis*, *P. gyrans* and *P. granifera*) but had not been retained as a marker of the genus. It turns out that with all strains of *Pavlova* for which we now have sections, this PY is a very distinctive feature of the genus.

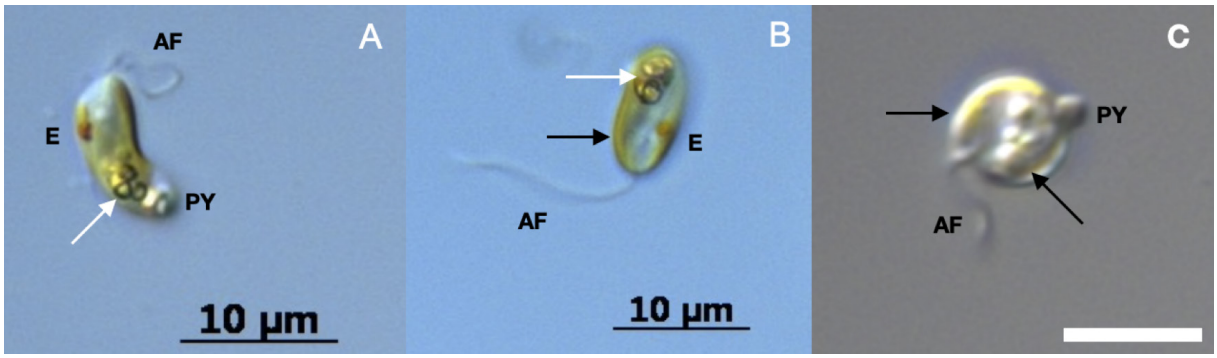

Fig. 10. *Pavlova* sp. AC248, motile cells, LM images. Side views of curved oblong (**A**), ovoid (**B**) and spherical (**C**) free-swimming cells with conspicuous S-shaped AF emerging apically. Greenish brown parietal C (black arrows) with an E and a posterior bulging PY. Vacuolar crystals of barium sulphate (white arrows). Scale bars = 10 µm.

Indeed, at the time of the revision of the species *P. pinguis*, Green (1980) observed this pyrenoid very clearly in posterior position which he described as "large and conspicuous, frequently being pushed into a bulge at the posterior end of the cell.". He also noted that this PY is "...frequently penetrated by a tubular invagination containing cytoplasmic material...". In fact, his illustrations (see his figs 8, 44, 45) clearly show the curved shape of this PY in *P. pinguis*, as does fig. 7F of Bendif *et al.* (2011). In their revision of *P. gyrans*, Green & Manton (1970) noted the central position of the PY within the C as well as its prominent bulging shape but did not examine thin-sections in TEM allowing them to see its curved shape. In their revision of the genus *Pavlova* they retained the fact that the C is bilobed with a prominent PY. Bendif *et al.* (2011) also showed this recurving PY in *P. gyrans* (see their fig. 6G) but retained only the bulge it forms on the cell. For *P. granifera*, Green (1973) showed the same shape and organisation of the PY (see his fig. 4) with an extension this time towards the interior of the cell (see his fig. 35), a situation we also observed only in the case of *Pavlova* AC250 (Fig. 13C). Green (1973) did not retain the singular shape of this PY but reports in his revision of the *P. granifera*, that the PY is "discretely

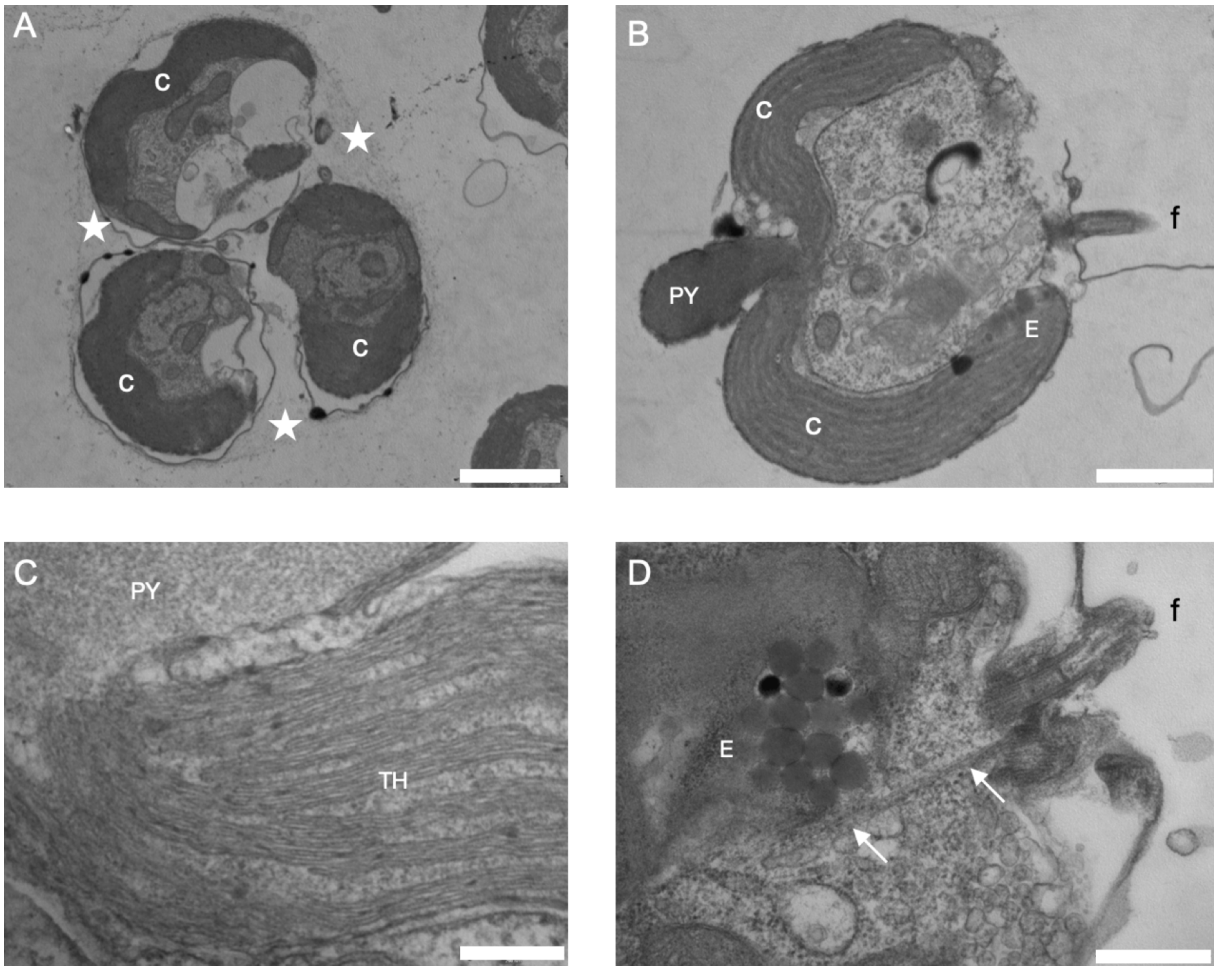

Fig. 11. *Pavlova* sp. AC248, chloroplast details, TEM images (Fix 1). **A**. Benthic colony of non-motile cells surrounded by a single, loose, non-layered M (white stars); single cup-shaped parietal C. **B**. Longitudinal section of a flagellate cell with parallel arrangement of TH in the C. Posterior PY protruding from the centre of the C, opposite a F, with an E at the tip of the C on its inner face. **C**. Detail of parallel TH lamellae forming stacks of 4 or 5 ending at the beginning of the PY.**D**. Detail of F insertion area showing proximity of the intrachloroplastic E to the long flagellar root (white arrows). Scale bars: A–B = 2 µm; C–D = 200 nm.

bulging towards the interior of the cell" (Green 1980). Bendif *et al.* (2011) also observe this pyrenoid in *P. granifera* but with less detail.

The singular shape of this PY that we describe as campylotropous is indeed a distinctive feature of the species of the genus *Pavlova* since in *Exanthemachrysis* (the other genus of Pavlovophyceae with a bulging pyrenoid) the two species now described do not show such a recurving shape, but a simple sphero-ovoid PY (see for *E. gayraliae*: Gayral & Fresnel 1979: figs 11–12, 21–22 and Bendif *et al.* 2011: fig. 4E; for *E. fresneliae* sp. nov.: Fig. 3).

When Butcher (1952) erected the genus *Pavlova*, he noted the presence of "leucosin bodies" in the posterior part of the cells and his drawings (see Butcher 1952: pl. II, figs 35–37) clearly show what is now known to be this type of PY. He did not retain this character as distinctive of the genus, nor did Green (1967), as cited above, when describing *P. pinguis* and his subsequent revision of the genus *Pavlova*. Bendif *et al.* (2011) introduced a more detailed description of the single C in their revised description by stating that it had a "posterior bulging pyrenoid and conspicuous eyespot on the inner surface near the flagellar pit".

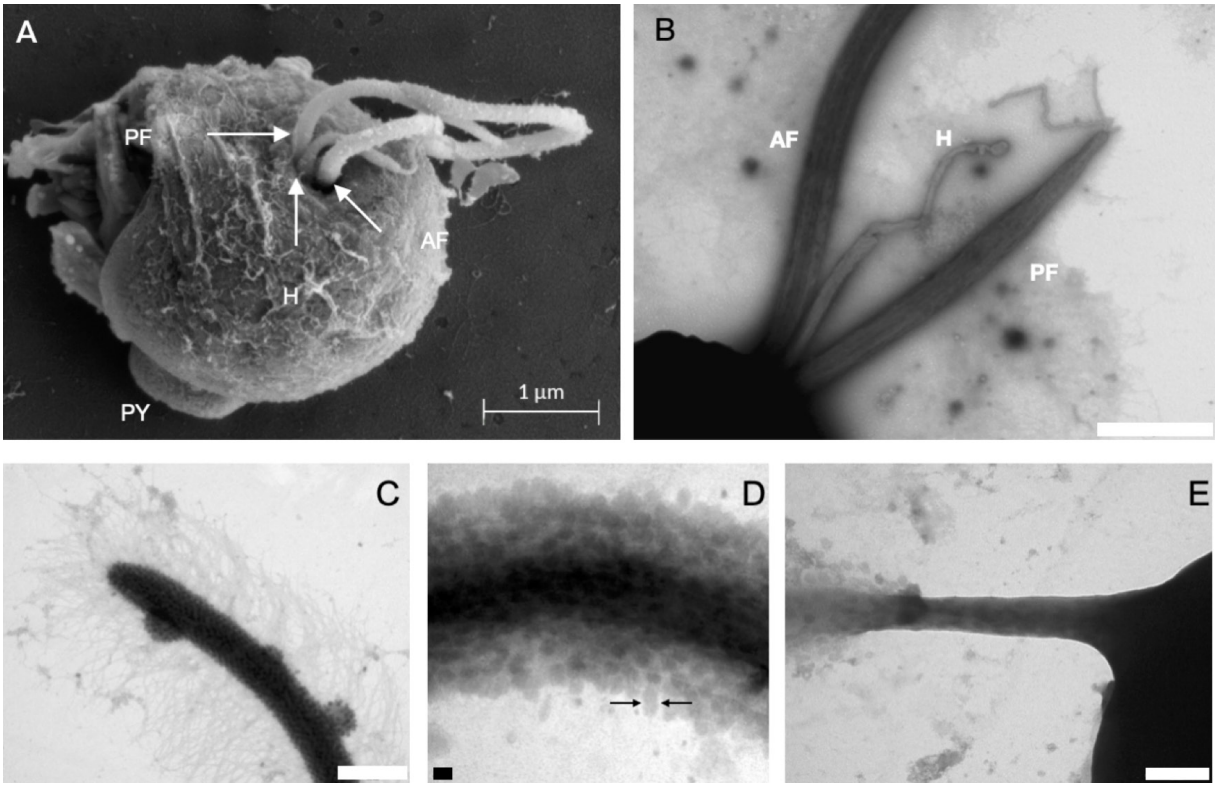

Fig. 12. *Pavlova* sp. AC248, flagellar apparatus details of motile cells. **A**. SEM image of apical view of a swimming cell with a complete F apparatus emerging almost in the centre of a narrow, shallow pit: tomentose S-shaped AF, end-tapered PF and bipartite H inserted between both. Bulging PY on the opposite side. **B–E**. Negative staining images. **B**. Details of the base of the F apparatus showing the AF, PF with a tapered end, and H consisting of a proximal part of constant diameter and a distal part of sub-equal length and smaller diameter. **C**. Distal rounded part of the AF (with a blistering of the membrane) showing covering of long non-tubular hairs and regular arrangement of KS. **D**. Central part of the AF showing flat KS with a slight median constriction (black arrows) arranged in several more or less regular layers. **E**. Proximal part of the AF with multilayered KS, extending after a bare area in the immediate vicinity of the cell. Scale bars: A–B = 1 µm; C = 0.5 µm; D = 50 nm; E = 200 nm.

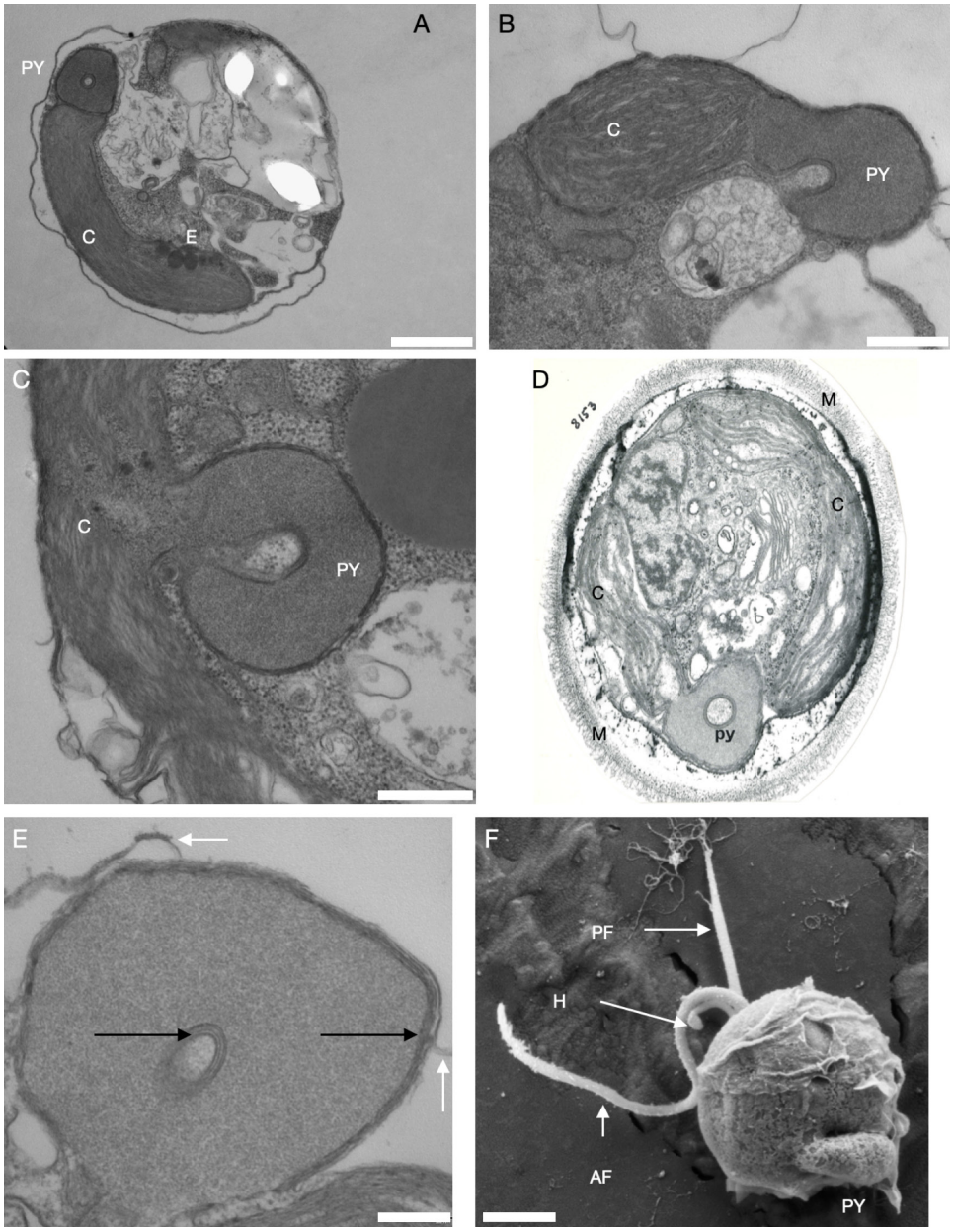

Fig. 13. Three *Pavlova* strains, details of the PY. **A–E**. TEM images. **A**. AC250, whole cell with a longitudinally sectioned C showing the E composed of osmiophilic clustered globules on its inner side and on the opposite side, the transversely sectioned campylotropous PY forming a slight hump on the cell surface and showing the narrow median space. (Fix 1). **B**. AC248, protruding campylotropous PY, longitudinally sectioned, completely surrounded by the C-membrane, bordered by periplastic ER on the cell surface and showing a narrow medial stromal space. (Fix 1). **C**. AC250, campylotropous PY, longitudinally sectioned emerging from the C towards the interior of the cell. (Fix 1). **D**. AC33, section of a palmelloid benthic cell surrounded by M with a cross sectioned campylotropous PY, in the middle of single cup-shaped parietal C, forming an ovoid bulge at the cell surface. (Original image, courtesy of C. Billard). **E**. AC248, detail of a cross section of the campylotropous pyrenoid attached to the plasma membrane (white arrows) showing the surrounding chloroplastic envelope lined on the inside by the periplastic ER (black arrows). (Fix 1). **F**. SEM image of AC248, postero-lateral view of a swimming cell with a complete F apparatus. PY bulging opposite the flagella with a tongue-like part projecting outwards from the cell. Scale bars: A = 1 µm; B = 20 nm; C = 0.5 µm; E = 200 nm; F = 2 µm.

Taxonomic outcome: a revised description of *Pavlova*

The particular and very characteristic shape of the pyrenoid in all species of *Pavlova* makes it a very distinctive feature that leads us to a revision of the genus description.

Pavlova Butcher emend. Véron
Fig. 13

Included species

Pavlova gyrans Butcher 1952: pl. II, figs 35–38.

Chrysocapsa granifera Mack 1954: fig. 1. – *Chrysocapsella granifera* (Mack) Bourrelly 1957. – *Pavlova granifera* (Mack) Green 1973.

Pavlova pinguis Green 1967: fig. 1.

Emended description

Motile, free-swimming, highly metabolic cells with two unequal flagella and a short haptonema. Longer anterior flagellum with fine non-tubular hairs and tiny knob-scales (i.e., 'dense bodies'), which may or may not be present on the cell body. A pit or canal penetrating the cell near the long anterior flagellum. Chloroplast with a central, large and campylotropous pyrenoid bulging posteriorly and a conspicuous E located on the inner side near the flagellar bases. Non-motile cells in unstratified mucilage with incomplete appendages.

Key to the genera

The hierarchisation of cytomorphological criteria to provide a simple key to the identification of taxa is not always easy. In his proposal based on characters of the motile cells, Green (1980) used the morphology of the flagella and haptonema as the first criterion, followed by the characters of the stigma, knob-scales, metabolism and the general shape of the cells. It appears today that the combined characters of the pyrenoid, the stigma and the thylakoids are sufficient to discriminate between the four genera (Fig. 14).

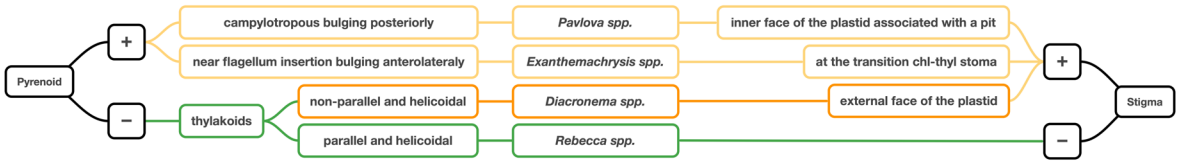

Fig. 14. Key to the genera of the Pavlovales (+ = present, - = absent). Drawn by A. Defrance.

Discussion

Comparison of *Exanthemachrysis fresneliae* sp. nov. with *E. gayraliae*

Exanthemachrysis fresneliae sp. nov. was isolated from a maceration of a stranded driftwood block collected on the mud on the lower shore of the Chausey Islands archipelago (Normandy, FR) and *E. gayraliae* from a mud maceration collected on the lower shore of the Orne River estuary (Lepailleur 1970). Apart from the mouth of the river Orne, these environments are comparable and both species present in this state a very predominant palmelloid stage. In culture, slow swimming cells (Fig. 1C–D) were obtained a few days after adding fresh culture medium, but these individuals very quickly become benthic again, each cell forming a new benthic colony by mitosis (Fig. 1A–B).

Considering that cell sizes can vary according to growth stages but also to mitotic phases, measurements must be taken cautiously and be done in optical microscopy (preparation techniques for SEM / TEM causing large size variations). As a result, *E. fresneliae* sp. nov. appears to be in the same size range as *E. gayraliae*, despite that cells are somewhat shorter and larger: palmelloid cells are 4.80 µm ± 0.57 long by 4.21 µm ± 0.56 wide while Lepailleur (1970) indicated 5–6 µm by 3.5–4 µm in *E. gayraliae*. Neither Gayral & Fresnel (1979) nor Bendif *et al.* (2011) measured palmelloid cells. Motile cells of *E. fresneliae* sp. nov. are much less rounded with a length (4.69 µm ± 0.61) similar to that measured for *E. gayraliae* (4–5.5 µm in Lepailleur 1970 and 4–5 µm in Gayral & Fresnel 1979) but unlike palmelloid cells, the motile cells are remarkably much slender (2.76 µm ± 0.35 large) compared to *E. gayraliae* (2–4 µm in Gayral & Fresnel 1979). The average of the individually calculated length / width ratios clearly confirms this peculiarity of cell dimorphism in *E. fresneliae* sp. nov. linked to life forms: 1.15 ± 0.13 (n = 50) for motile vs 1.72 ± 0.26 (n = 51) for non-motile cells.

The flagellate cells of *E. fresneliae* sp. nov. with their distinct covering of ovoid pedunculated KS (Figs 4–5) produced in the Golgi body (Fig. 5C) as confirmed here, clearly differ from *E. gayraliae* for which Gayral & Fresnel (1979) pointed out the absence of dense 'deposits' in the vesicles of the Golgi body. *Exanthemachrysis gayraliae*, represented by only one (type-) strain in all referenced culture collections, has been investigated three times by Lepailleur (1970), Gayral & Fresnel (1979) and Bendif *et al.* (2011) and KS were never seen. Apart from the remarkable presence of KS only in *E. fresneliae* sp. nov., the flagellar appendages apparatuses of the two species do not differ greatly, except that the AF appears to be longer in *E. gayraliae*. The M of the benthic stage is homogenous around *E. fresneliae* sp. nov. sister cells (Fig. 1A–B) which retain the bases of the flagellar apparatus (Fig. 2), contrary to what Lepailleur (1970) and Gayral & Fresnel (1979) reported for in *E. gayraliae*, insisting on the 'true' palmelloid stage as opposed to the pseudo-palmelloid stages of some other Pavlovophyceae. In both species, the single C shows helicoidal and parallel TH arrangements (Fig. 2) and a discreet E is located at the transition area between the TH and the bulging PY (Fig. 3). In *E. gayraliae*, the PY is located in the middle of the C (Gayral & Fresnel 1979) whereas in *E. fresneliae* sp. nov. it bulges at the terminal part of the C (Figs 2–3).

Special note on viral inclusions

Gayral & Fresnel (1979) demonstrated the presence of viral inclusions composed of 150–170 nm hexagonal particles in cells of *E. gayraliae* with a highly altered or even completely lysed C and where the N had completely disappeared. It is noteworthy that some non-motile N-lysed *E. fresneliae* sp. nov. cells also showed signs of viral infection with a cytoplasmic viroplasm (Fig. 6) composed of 50 nm virus particles (Fig. 6B). While the size and shape (icosahedral) of the virus particles seen in *E. gayraliae* suggest that it could be a Phycodnaviridae or a Mimiviridae / Mesomimiviridae, the particles in *E. fresneliae* sp. nov. are much smaller and the cross-sectional shape is less clearly hexagonal and appears to be ovoid or pentahedral (Fig. 6B). They could be a type of Picornavirales such as already found in *Heterosigma akashiwo* (Hada) Hada (Tai *et al.* 2003), in *Rhizosolenia setigera* Brightwell (Nagasaki *et al.* 2004) or a

Reoviridae also found in another unicellular alga *Micromonas pusilla* (Butcher) Manton & Parke (Attoui *et al.* 2006). Viroplasms have been found in *D. virescens* as reported by Zingone (1995).

Comparison of *Rebecca billardiae* sp. nov. with *R. salina* and *R. helicata*

Rebecca billardiae sp. nov. was isolated from a surface / sub-surface water sample in a highly turbulent area of the silt plug in the temperate macrotidal estuary of the Vire river, FR (station ESTUARY in Bazin *et al.* 2014) whose natural banks are lined with grassy meadows regularly submerged by the waves and artificial banks of piled up granite blocks. *Rebecca salina* (as *Pavlova mesolychnon* van der Veer) was isolated from a sandy mud sample collected in a salt-marsh far upstream from the mouth of the Lynher River estuary, Cornwall, UK (Van der Veer 1969, 1979) and *R. helicata* (as *P. helicata*) from seawater up-taken on a flooded halophyte meadow of the island Schiermonnikoog, NL (Van der Veer 1972, 1979). It thus seems, judging from the habitats of the three species now described, that the genus *Rebecca* is particularly fond of upstream zones of estuaries with a muddy benthos covered with halophytes. This corroborates the observations detailed by Carter (1937) who described *R. salina* (as *Nephrochloris salina* Carter) from a small brackish pool at Bembridge (Isle of Wight, UK) surrounded by "…grassy vegetation with rough weeds and shrubs…a ditch largely choked with *Spartina townsendii*… clumps of *Juncus maritimus*".

While Carter (1937) reported palmelloid stages becoming slightly amoeboid without flagella in *R. salina*, these were never observed in *P. mesolychnon* (van der Veer 1969, 1979) nor by Green (1976) or Bendif *et al.* (2011) during re-examinations, nor in *P. helicata* (van der Veer 1972, 1979). Logically, Green (in Edvardsen *et al.* 2000) did not retain this character by making *Rebecca* an exclusively motile genus. We therefore consider that the non-swimming cells observed here, clustering closely and retaining their twisted AF and not surrounding themselves with M (Fig. 7A) correspond to the substrate-attached cells that van der Veer (1972) observed. Green (1980) potentially associated this peculiar state of the cells with a response to environmental conditions.

The genus *Rebecca* is described as featuring elongate and slightly compressed cells (Edvardsen *et al.* 2000), *R. salina* stated as oval, obovate, ovate, pyriform and variable by Carter (1937) and van der Veer (1969) or oval to oblong by Bendif *et al.* (2011), while *R. helicata* is described in similar terms to which van der Veer (1972) added circular, and on the front end ventrally truncated cells. *Rebecca billardiae* sp. nov. varies from those listed forms (Fig. 7) also having a cubic shape (Fig. 9A) but mainly features cells with unequal flat faces forming acute or obtuse protruding angles (Figs 7A–B, 8A–B, 9B) looking quite similar (except here all sides of the cells are taken into account) to the observations of van der Veer (1972). Angular cells in *R. billardiae* sp. nov., unlike other cells, are not metabolic; the other two species of *Rebecca* are not metabolic either. Although not flattened, the sizes (length and width) of the cells of the new species are comparable to those of the two other species of *Rebecca* (van der Veer 1972; Green 1976). Long and posterior beaded branched filipodia are present in all three species. The body-scales defined as club-shaped in *R. helicata* and *R. salina* (Green 1976) resemble, in *R. billardiae* sp. nov., the flagellar KS of these two species but with only one constriction (Fig. 9G), as opposed to two.

The area of flagellar insertion is identical in all three species (ventral sub-apical in a depression), but here we show a sinus of the superficial pit around a column containing the haptonemal and flagellar base sheathed by a cytoplasmic layer surrounded by the plasma membrane (Fig. 8C). The length of the AF is within the range of dimensions given for the other two species, although that of *R. helicata* appears to be somewhat longer. The presence of hairs, visible in *R. salina*, was not observed in *R. helicata* or *R. billardiae* sp. nov., but in the latter this distally attenuated AF is covered by a thick layer of KS in regular rows (Fig. 9G) extending after a bare proximal area (Fig. 9F) in the immediate vicinity of the cell. These KS are pedunculated, ovoid to clavate, showing a very slight median constriction (Fig. 9G). As in the other two species of *Rebecca*, the PF is vestigial and is here sporadically covered with KS identical

to those of the AF (Fig. 8H). The bipartite H, with a proximal part of constant diameter and a distal part with a pearl necklace structure, is comparable in total length to that measured in *R. salina* but slightly smaller than in *R. helicata.*

The single golden-brown C in *R. billardiae* sp. nov. (Fig. 7) is bilobed showing a parallel, helicoidal arrangement of thylakoids (Fig. 8B), without E or PY as in *R. salina*. The suspicion of the absence of a pyrenoid in *R. helicata* raised by Bendif *et al.* (2011) is reinforced. We therefore rule that these characters are identical within the genus *Rebecca*.

On the apparent complexity of a highly sequenced genus with few species: *Pavlova*

While the study of Bendif *et al.* (2011) demonstrated a clear separation between genera *Diacronema* and *Pavlova* (clades 4 and 3, respectively), it also revealed a hitherto unsuspected complexity within clade 3 that is unexplained despite it being the richest clade in terms of the number of available sequences but perhaps very poor in terms of species. As their sub-clade 3.1 contains the traceable type-strains of *P. pinguis* and *P. gyrans*, our investigation focused here on clade 3.2 which shows a greater diversity and a clear pattern with two sub-subclades, one featuring the type-strain of *P. granifera* (freshwater) and the other marine strains never investigated before (AC19 – see above, AC248 and AC250 for those preserved by AC). The genus *Pavlova* is notable in having, together with the genus *Diacronema*, only one freshwater species, namely *P. granifera*. The issue of habitats was raised by Bendif *et al.* (2011) as a potential indicator of speciation between sub-clades. Life forms in the pavlovophytes could also be related to possible life cycles.

Butcher (1952) in his description of *P. gyrans* only states that the strain was isolated from the River Helford, Cornwall (UK), which confirms its brackish nature. He notes that in culture, a palmelloid stage is occasionally seen, whereas Green & Manton (1970), in a detailed examination of the same isolate, indicated that they did not observe forms other than motile stages, a feature they repeated in their revised description of the species. Also Bendif *et al.* (2011) did not mention a non-motile stage in their study of *P. gyrans*. The second species, *P. pinguis*, is purely marine, isolated off Madeira Island (PT). An alternation of pelagic and benthic stages (motile vs non-motile) was observed, with both stages undergoing mitosis. The benthic stage is typically a palmelloid one as surrounded by M and lacking F (Green 1967). Bendif *et al.* (2011) observed exclusively the flagellated stage.

To our knowledge, only two properly referenced isolates of *P. granifera* (as *Chrysocapsa granifera* Mack) have been recorded: by Mack (1954) from a mud flake adhering to *Myriophyllum spicatum* L. collected in Lake Neusiedl (AT) and by Geitler (1969) from a small multi-layered mass growing on various organic residuals (plant debris, pieces of wood, insect larvae skins, bird feathers, filamentous algae) in Lake Lunzer (AT). In 1971, Geitler stated that in addition to its massive growth forming zonal belts, *P. granifera* in the epilithic stage is able to withstand desiccation in temperate conditions. He also states that it can form temporary and localised zones. In 1972, Tschermak-Woess (despite the confusion in her paper (see Green 1973 and Tschermak-Woess 1979) confirmed the presence of this species as an epiphyte. A true microphytoepibenthic (epi-phytic, -zootic and -lithic) with a palmelloid stage of this species is thus proven. This is also the case for the Mediterranean marine strain *Pavlova* AC33 revealed to be very close to *P. granifera*, isolated from driftwood off the Mediterranean coast of Tartous (SY), which forms a loose but well-defined mucilaginous envelope within which cells (up to several hundred) divide and from which motile cells emerge when fresh culture medium is added (Billard C., pers. comm.).

Strain AC248 was isolated in the spring of 1978 from a benthic sample of a puddle on the rocky Mediterranean coast of the island of Saint-Honorat (FR) and strain AC250 in the same period from the urbanised continental Mediterranean coast of the marina of the town of Menton (FR). They both show a non-motile benthic stage that does not form colonies (no sister-cell figures observed) but rather an

agglutination of cells, ceasing to swim while retaining their incomplete flagellar apparatus and surrounding themselves with a light, non-stratified M: this stage qualified as pseudo-palmelloid since we did not observe true palmelloid colonies in these two strains.

In short, it is not obvious to relate a cell stage to a living environment. Authentic palmelloid stages are found in *P. pinguis*, *P. granifera* and AC33, which are isolated from marine, freshwater continental and coastal environments, respectively. Conversely, the palmelloid stage is less structured or even occasional in the coastal and brackish *Pavlova* strains AC248, AC250 and *P. gyrans*. However, the lack of precise data on sample location or description of sampling environments, combined with the sampling bias due to the often manual collection in marine sublittoral areas or coastal lakes could lead to over-interpretation. Studies of phase change conditions would be necessary to better understand the modalities and infer them to life stages. Similarly, the fact that strains AC248 and AC250 are morphologically indistinguishable from other *Pavlova* species only reinforces the conclusion made by Bendif *et al.* (2011) that there is evidence of cryptic entities within the genus *Pavlova*, which nevertheless remains well defined.

Acknowledgments

The authors are grateful to their colleagues at the Université de Caen Normandie: Bertrand Le Roy is warmly thanked for his meticulous care in maintaining the cultures at Algobank-Caen as well as to the samples collectors and strains isolators without whom nothing would be possible; Prof. Marie-Agnès Lucas-Avenel of the Latin Institute for her valuable advice of the Latin epithets; Chantal Billard and Jacqueline Fresnel for their always valuable advice and their numerous linguistic corrections. They would also like to thank the European Erasmus "Lifelong Learning" programme for having allowed the mobility of Anthony Taylor from the University of Portsmouth to the Université de Caen Normandie. A. Defrance is thanked for his help in formatting the figures and for the drawing of Fig. 14. Finally, special thanks to Michael D. Guiry and his team at the National University of Ireland whose database www.algaebase.org is such a valuable resource.

References

Attoui H., Jaafar F.M., Belhouchet M., de Micco P., de Lamballerie X. & Brussaard C.P.D. 2006. *Micromonas pusilla* reovirus: a new member of the family Reoviridae assigned to a novel proposed genus (*Mimoreovirus*). *Journal of General Virology* 87 (5):1375–1383. https://doi.org/10.1099/vir.0.81584-0

Bazin P., Jouenne F., Friedl T., Deton-Cabanillas A.-F., Le Roy B. & Véron B. 2014. Phytoplankton diversity and community composition along the estuarine gradient of a temperate macrotidal ecosystem: Combined morphological and molecular approaches. *PLoS ONE* 9 (4): e94110. https://doi.org/10.1371/journal.pone.0094110

Bendif E.L., Probert I., Hervé A., Billard C., Goux D., Lelong C., Cadoret J.-P. & Véron B. 2011. Integrative taxonomy of the Pavlovophyceae (Haptophyta): A reassessment. *Protist* 162: 738–761. https://doi.org/10.1016/j.protis.2011.05.001

Bourrelly P. 1957. Recherches sur les Chrysophycées. Morphologie, phylogénie, systématique. *Revue Algologique – Mémoire Hors-Série* 1: 1-412

Butcher R.W. 1952. Contributions to our knowledge of the smaller marine algae. *Journal of the Marine Biological Association of the United Kingdom* 31: 175–191. https://doi.org/10.1017/S0025315400003751

Carter N. 1937. New and interesting algae from brackish water. *Archiv für Protistenkunde* 90: 1–68.

Cosson J. 1987. Croissance des sporophytes résultats d'hybridations interspécifiques et intergénérique chez les laminaires. *Crytogamie, Algologie* 8: 61–72.

Edvardsen B., Eikrem W., Green J.C., Andersen R.A., Moon-van-der-Staay S.Y. & Medlin L.K. 2000. Phylogenetic reconstructions of the Haptophyta inferred from 18S ribosomal DNA sequences and available morphological data. *Phycologia* 39: 19–35. https://doi.org/10.2216/i0031-8884-39-1-19.1

Edvardsen B., Egge E.S. & Vaulot D. 2016. Diversity and distribution of haptophytes revealed by environmental sequencing and metabarcoding – a review. *Perspectives in Phycology* 3: 77–91. https://doi.org/10.1127/pip/2016/0052

Egge E.S., Johannessen T.V., Andersen T., Eikrem W., Bittner L., Larsen A., Sandaa R.A. & Edvardsen B. 2015. Seasonal diversity and dynamics of haptophytes in the Skagerrak, Norway, explored by high-throughput sequencing. *Molecular ecology* 24: 3026–3042. https://doi.org/10.1111/mec.13160

Eikrem W., Medlin L., Hendriks J., Rokitta S., Rost B., Probert I., Throndsen J. & Edvardsen B. 2017. Haptophyta. *In*: Archibald J.M., Simpson A.G.B, Slamovits C.H., Margulis L., Melkonian M., Chapman D.J. & Corliss J.O. (eds) *Handbook of the Protists*: 1–61. Springer, Cham. https://doi.org/10.1007/978-3-319-32669-6_38-2

Gayral P. & Fresnel J. 1979. *Exanthemachrysis gayraliae* Lepailleur (Prymnesiophyceae, Pavlovales): Ultrastructure et discussion taxinomique. *Protistologica* XV: 271–282.

Geitler L. 1969. Beobachtungne über *Chrysocapsella granifera*. *Österreichische botanische Zeitschrift* 117: 365–371. https://doi.org/10.1007/BF01377794

Geitler L. 1971. Weitere Untersuchungen über ein Massenvorkommen von *Chrysocapsella granifera* im Linzer Unteresee mit Zonenbildung. *Archiv für Hydrobiologie* 68: 516–518.

Green J.C. 1967. A new species of *Pavlova* from Madeira. *British Phycological Bulletin* 3: 299–303. https://doi.org/10.1080/00071616700650181

Green J.C. 1973. Studies in the fine structure and taxonomy of flagellates in the genus *Pavlova*. II. A freshwater representative, *Pavlova granifera* (Mack) comb. nov. *British Phycological Journal* 8: 1–12. https://doi.org/10.1080/00071617300650011

Green J.C. 1976. Notes on the flagellar apparatus and taxonomy of *Pavlova mesolychnon* Van der Veer, and on the status of *Pavlova* Butcher and related genera within the Haptophyceae. *Journal of the Marine Biological Association of the United Kingdom* 56: 595–602. https://doi.org/10.1017/S0025315400020671

Green J.C. 1980. The fine structure of *Pavlova pinguis* Green and a preliminary survey of the order Pavlovales (Prymnesiophyceae). *British Phycological Journal* 15: 151–191. https://doi.org/10.1080/00071618000650171

Green J.C. & Manton I. 1970. Studies in the fine structure and taxonomy of the flagellates in the genus *Pavlova* I. A revision of *Pavlova gyrans*, the type species. *Journal of the Marine Biological Association of the United Kingdom* 50: 1113–1130. https://doi.org/10.1017/S0025315400005981

Guillard R.R.L. & Ryther J.H. 1962. Studies of marine planktonic diatoms. 1. *Cyclotella nana* Hustedt and *Detonula confaervacea* Cleve. *Canadian Journal of Microbiology* 8: 229–239. https://doi.org/10.1139/m62-029

Jones H.L.J., Leadbeater B.S.C. & Green J.C. 1994. Mixotrophy in prymnesiophytes. *In*: Green J.C. & Leadbeater B.S.C. (eds) *The Haptophyte Algae*: 247–263. Systematics Association Special, 51. Clarendon Press, Oxford.

Jordan R.W., Cros L. & Young J.R. 2004. A revised classification scheme for living haptophytes. *Micropaleontology* 55 (Suppl. 1): 55–79. https://doi.org/10.2113/50.Suppl_1.55

Kawachi M., Nakayama T., Kayama M., Tomura M., Miyashita H., Bojo O., Rhodes L., Rym S., Pienaar R.N., Probert I., Inouye I. & Kamikawa R. 2021. Rappemonds are haptophyte phytoplankton. *Current Biology* 31: 1–9. https://doi.org/10.1016/j.cub.2021.03.012

Lepailleur H. 1970. Sur un nouveau genre de Chrysophycées: *Exanthemachrysis* nov. gen. (*E. gayralii* nov. sp.). *Comptes Rendus de l'Académie des sciences Paris* 270 : 928-931.

Mack B. 1954. Untersuchungen an Chrysophyceen. V–VII. *Österreichische botanische Zeitschrift* 101: 64–73. https://doi.org/10.1007/BF01283604

Nagasaki K., Tomaru Y., Katanozaka N., Shirai Y., Nishida K., Itakura S. & Yamaguchi M. 2004. Isolation and characterization of a novel single-stranded RNA virus infecting the bloom-forming diatom *Rhizosolenia setigera*. *Applied and Environmental Microbiology* 70 (2): 704–711. https://doi.org/10.1128/AEM.70.2.704-711.2004

Not F., Siano R., Koistra W.H.C.F., Simon N., Vaulot D. & Probert I. 2012. Diversity and ecology of eukaryotic marine phytoplankton. *Advances in Botanical Research* 64: 1–53. Academic Press, Cambridge. https://doi.org/10.1016/B978-0-12-391499-6.00001-3

Parke M., Manton I. & Clarke B. 1955. Studies on marine flagellates. II. Three new species of *Chrysochromulina*. *Journal of the Marine Biological Association of the United Kingdom* 34: 579–609. https://doi.org/10.1017/S0025315400008833

Plancq J., Couto J., Ijaz U.Z., Leavitt P.R. & Toney J. 2019. Next generation sequencing to identify lacustrine haptophytes in the Canadian Prairies: significance for temperature proxy applications. *Journal of Geophysical Research: Biogeosciences* 124: 2144–2158. https://doi.org/10.1029/2018JG004954

Ponis E., Probert I., Véron B., Le Coz J.R., Mathieu M. & Robert R. 2006. Nutritional value of six Pavlovophyceae for *Crassostrea gigas* and *Pecten maximus* larvae. *Aquaculture* 254: 544–553. https://doi.org/10.1016/j.aquaculture.2005.11.017

Shalchian-Tabrizi K., Reier-Røberg K., Ree D.K., Klaveness D. & Bråte J. 2011. Marine-freshwater colonizations of Haptophytes inferred from phylogeny of environmental 18S rDNA sequences. *Journal of Eukaryotic Microbiology* 58: 315–318. https://doi.org/10.1111/j.1550-7408.2011.00547.x

Simon M., Lopez-Garcia P., Moreira D. & Jardillier L. 2013. New haptophyte lineages and multiple independent colonizations of freshwater ecosystems. *Environmental Microbiology Reports* 5: 322–32. https://doi.org/10.1111/1758-2229.12023

Strassert J.F.H., Irisarri I., Williams T.A. & Burki F. 2021. A molecular timescale for eukaryote evolution with implications for the origin of red algal-derived plastids. *Nature Communications* 12: 1879. https://doi.org/10.1038/s41467-021-22044-z

Tai V., Lawrence J.E., Lang A.S., Chan A.M., Culley A.I. & Suttle C.A. 2003. Characterization of HaRNAV, a single-strandedRNA virus causing lysis of *Heterosigma akashiwo* (Raphidophyceae). *Journal of Phycology* 39: 343–352. https://doi.org/10.1046/j.1529-8817.2003.01162.x

Tschermak-Woess E. 1972. Über die Haptophycee *Sarcinochrysis granifera* aus dem Neusiedlersee. *Österreichische botanische Zeitschrift* 121: 235–255. https://doi.org/10.1007/BF01373377

Tschermak-Woess E. 1979. Richtigllung betreffend *Sarcinochrysis granifera* (Mack) Tsch.-Woess (Prymnesiophyceae). *Plant Systematics and Evolution* 132: 343–345. https://doi.org/10.1007/BF00982397

van der Veer J. 1969. *Pavlova mesolychnon* (Chrysophyta) a new species from the Tamar estuary, Cornwall. *Acta Botanica Neerlandica* 18 (4): 496–510. https://doi.org/10.1111/j.1438-8677.1969.tb00590.x

van der Veer J. 1972. *Pavlova helicata* (Haptophyceae), a new species from the Frisian Island Schiermonnnikoog, the Neverthlands. *Nova Hedwigia* 23: 131–159.

van der Veer J. 1979. Pavlova and the taxonomy of flagellates, especially the Chrysomonads. PhD Thesis, Rijks-universiteit, Groningen, The Netherlands.

Zhang X., Yang S., Sun J., Qiao Y., Wang J. & Liu H. 2018. The first record of *Pavlova pinguis* (Pavlovophyceae, Haptophyta) in China Seas. *Acta Oceanologica Sinica* 37: 28–32. https://doi.org/10.1007/s13131-018-1294-1

Zingone A. 1995. The role of viruses in the dynamics of phytoplankton blooms. *Giornale botanico italiano* 129: 415–423. https://doi.org/10.1080/11263509509436155

Manuscript received: 2 May 2022
Manuscript accepted: 14 October 2022
Published on: 8 March 2023
Topic editor: Frederik Leliaert
Desk editor: Radka Rosenbaumová